Supplementary Material

Fabrication of Silk Sericin-Anthocyanin Nanocoating for Chelating and Saturation-Visualization Detection of Metal Ions

Liang Yao, [a, 1] Minglu Hao, [b, 1] Feng Zhao, [c] Yilin Wang, [d] Yueru Zhou, [c] Zhongyi Liu, [c] Xiaofan An, [b] Zhongfeng Gao, [b] Jun Wang, [a] Tao Zheng, [e] Pu Chen, [b, c, *] and Lei Zhang [c, *]

[a] School of Biotechnology and Sericultural Research Institute, Jiangsu University of Science and Technology, Zhenjiang, Jiangsu 212018, China

[b] School of Advanced Materials Institute, Qilu University of Technology, Shandong Academy of Sciences, Jinan 250014, China

[c] Department of Chemical Engineering and Waterloo Institute for Nanotechnology, University of Waterloo, Waterloo, Ontario, Canada, N2L 3G1

[d] Institute of Translational Medicine, Zhejiang University, Hangzhou, Zhejiang 310029, China

[e] Guangzhou Institute of Energy Conversion, Chinese Academy of Sciences, Guangzhou, China, 510640

Corresponding Authors:

Department of Chemical Engineering and Waterloo Institute for Nanotechnology, University of Waterloo, Waterloo, Ontario, Canada, N2L 3G1

* E-mail: l78zhang@uwaterloo.ca (L. Zhang) & p4chen@uwaterloo.ca (P. Chen)

[1] These authors contributed equally.

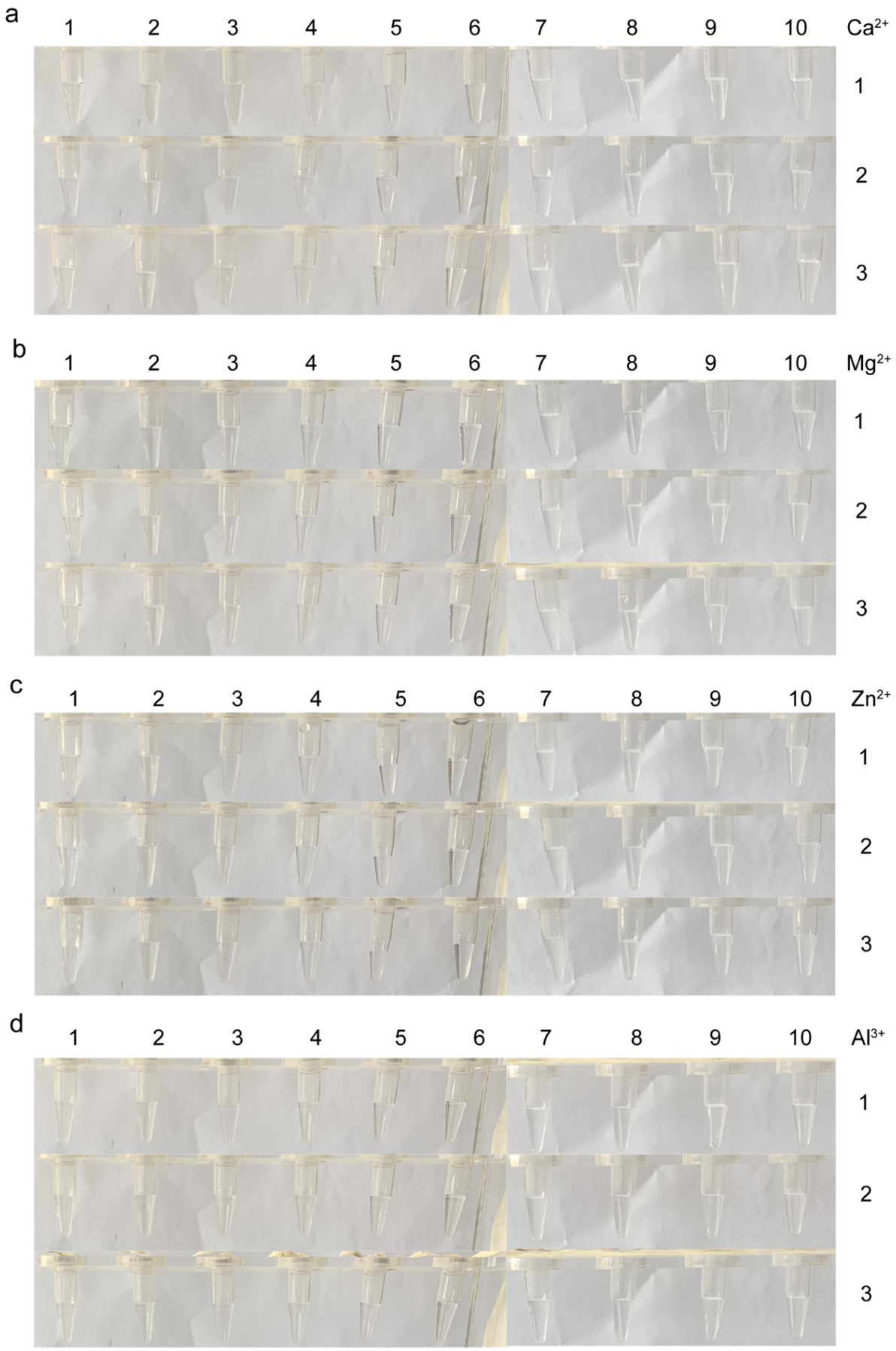

Fig. S1 Images of different concentrations of (a) Ca^{2+}, (b) Mg^{2+}, (c) Zn^{2+}, and (d) Al^{3+} solution.

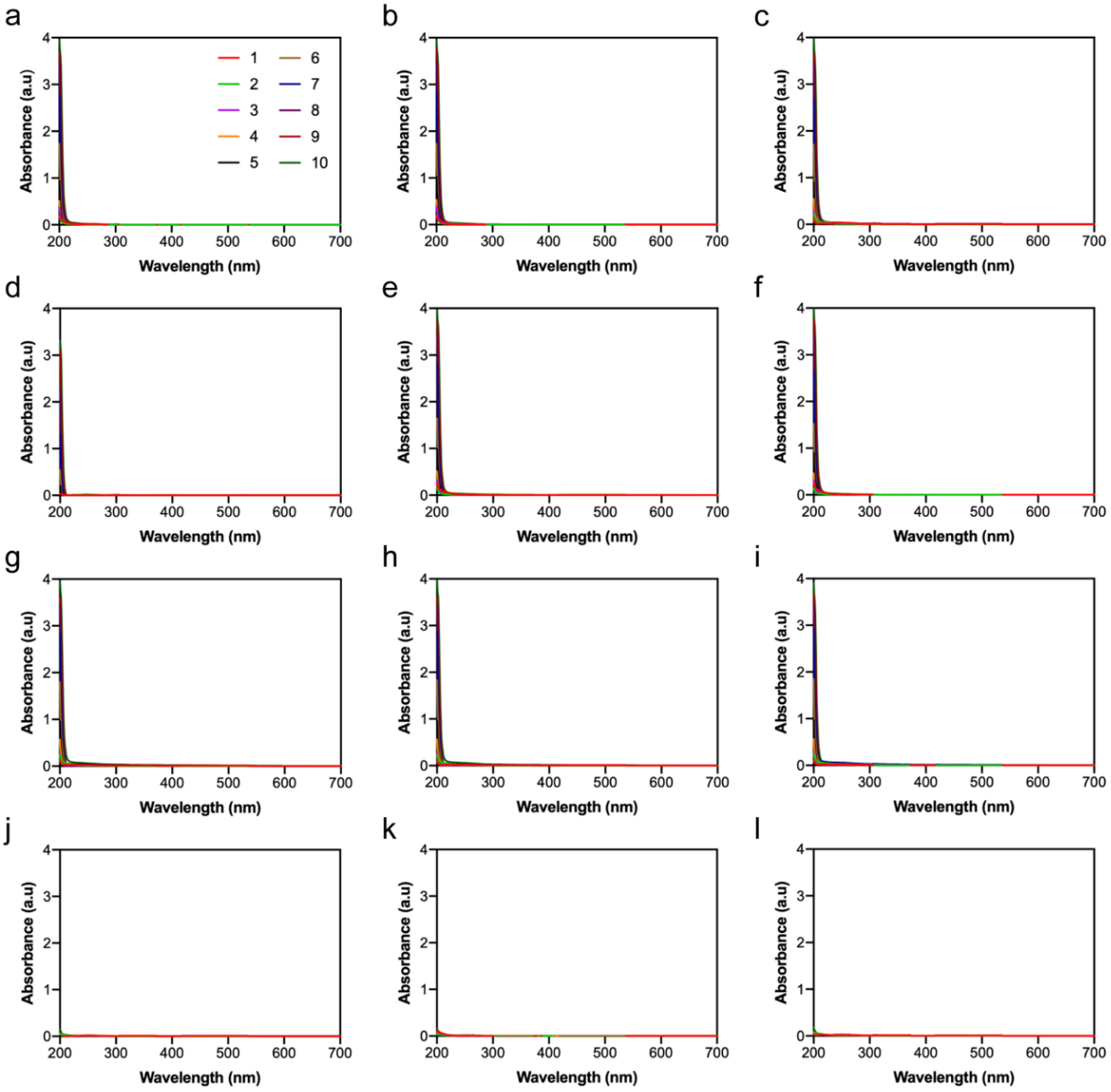

Fig. S2 UV-Vis absorbance of different concentrations of (a-c) Ca^{2+}, (d-f) Mg^{2+}, (g-i) Zn^{2+}, and (j-i) Al^{3+}.

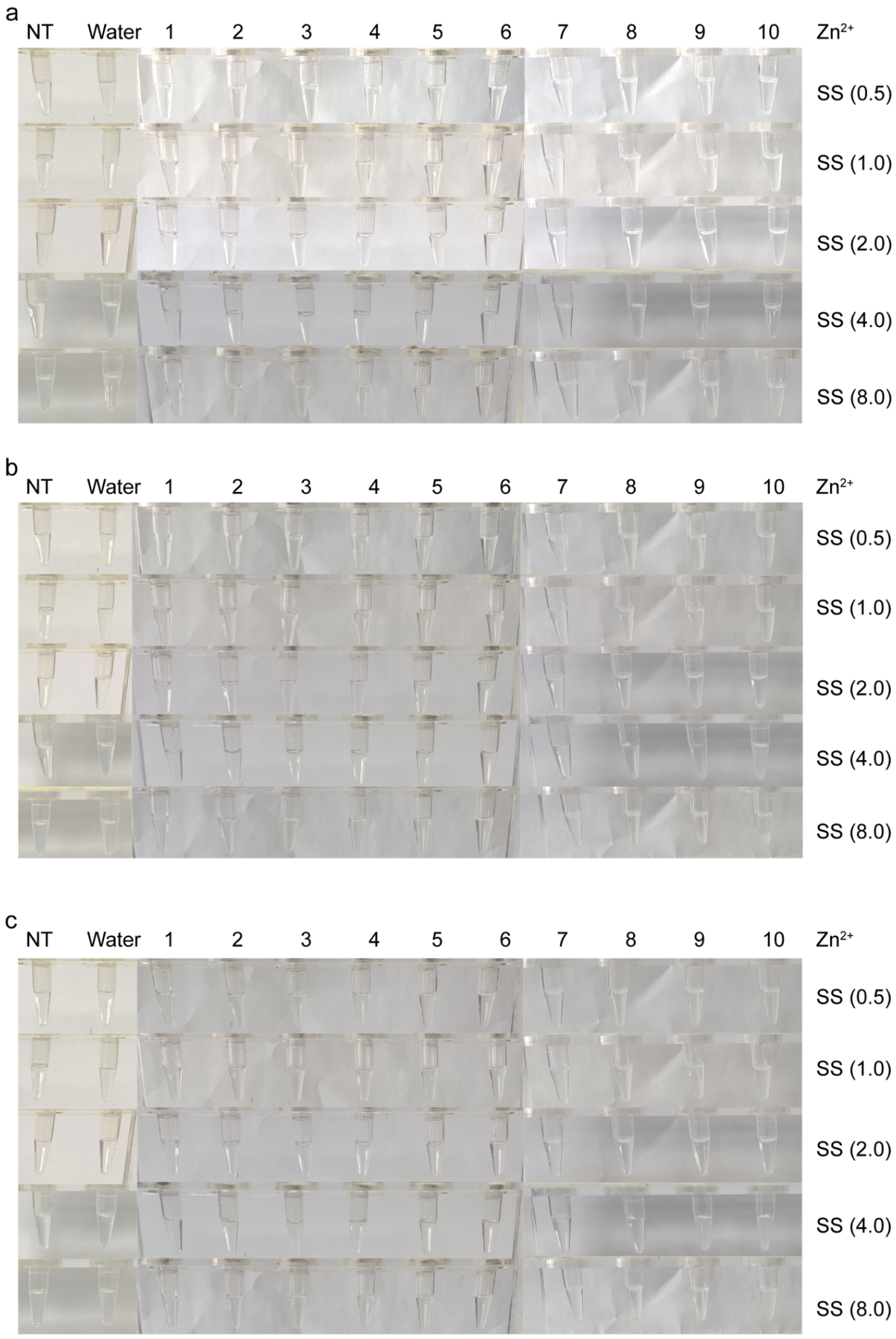

Fig. S3 Images of different concentrations of SS mixed with Zn^{2+}.

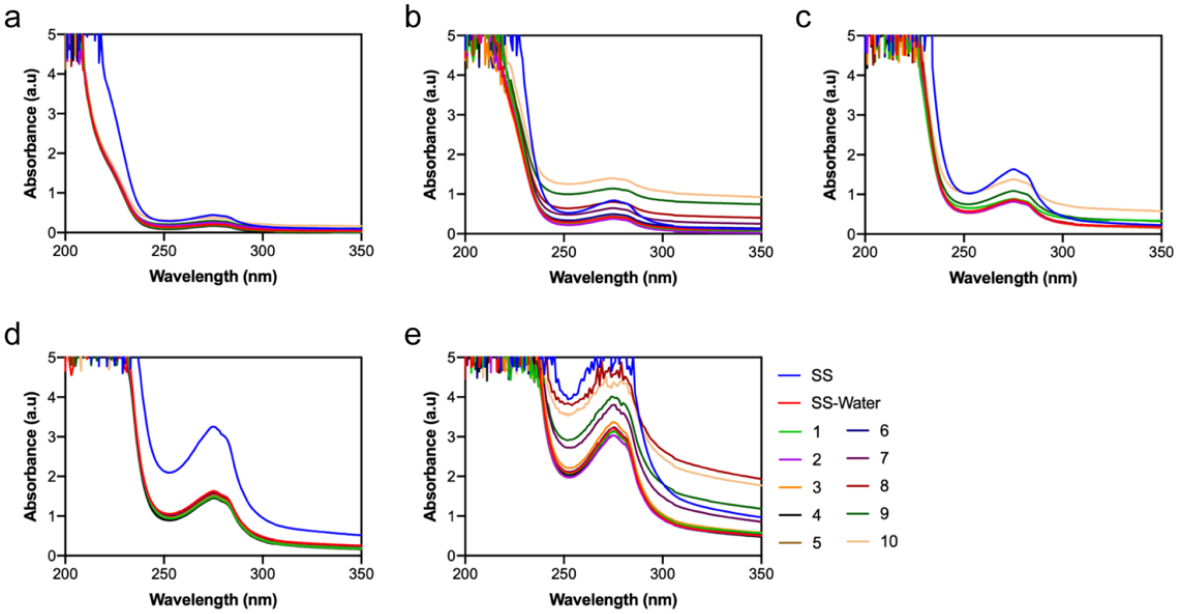

Fig. S4 UV-Vis absorbance of (a) SS (0.5), (b) SS (1.0), (c) SS (2.0), (d) SS (4.0), and (e) SS (8.0) mixed with Zn^{2+} (Test 1).

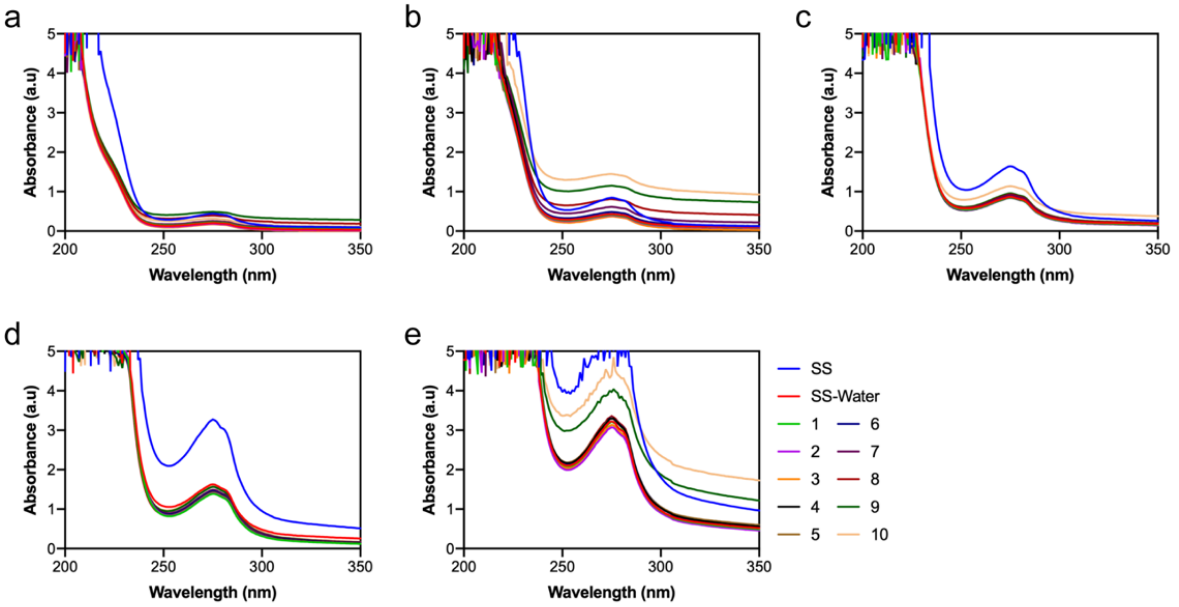

Fig. S5 UV-Vis absorbance of (a) SS (0.5), (b) SS (1.0), (c) SS (2.0), (d) SS (4.0), and (e) SS (8.0) mixed with Zn^{2+} (Test 2).

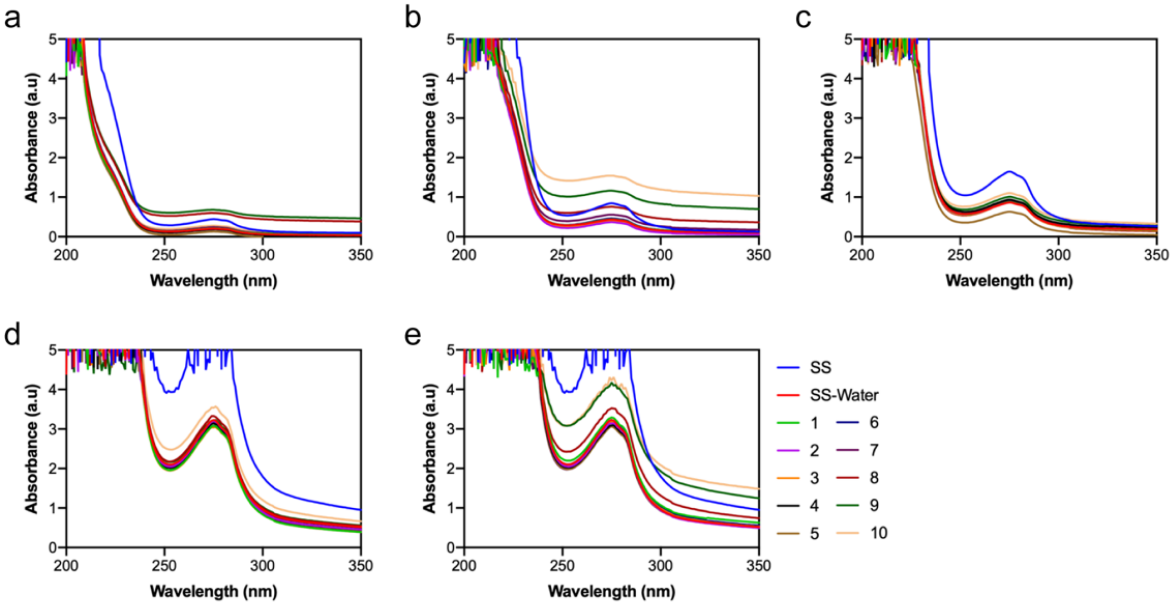

Fig. S6 UV-Vis absorbance of (a) SS (0.5), (b) SS (1.0), (c) SS (2.0), (d) SS (4.0), and (e) SS (8.0) mixed with Zn^{2+} (Test 3).

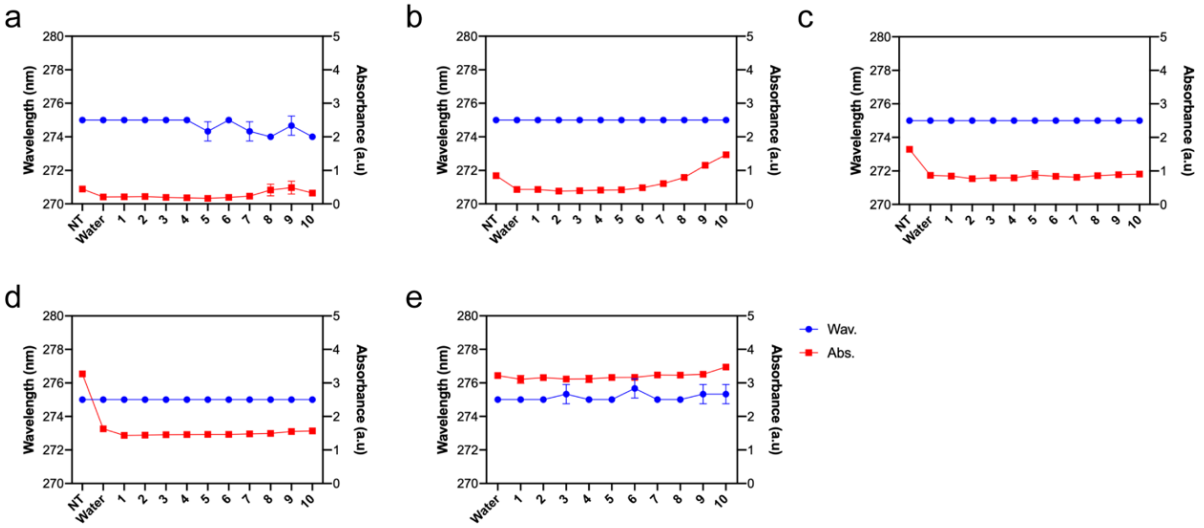

Fig. S7 UV-Vis absorbance change of (a) SS (0.5), (b) SS (1.0), (c) SS (2.0), (d) SS (4.0), and (e) SS (8.0) mixed with Zn^{2+}.

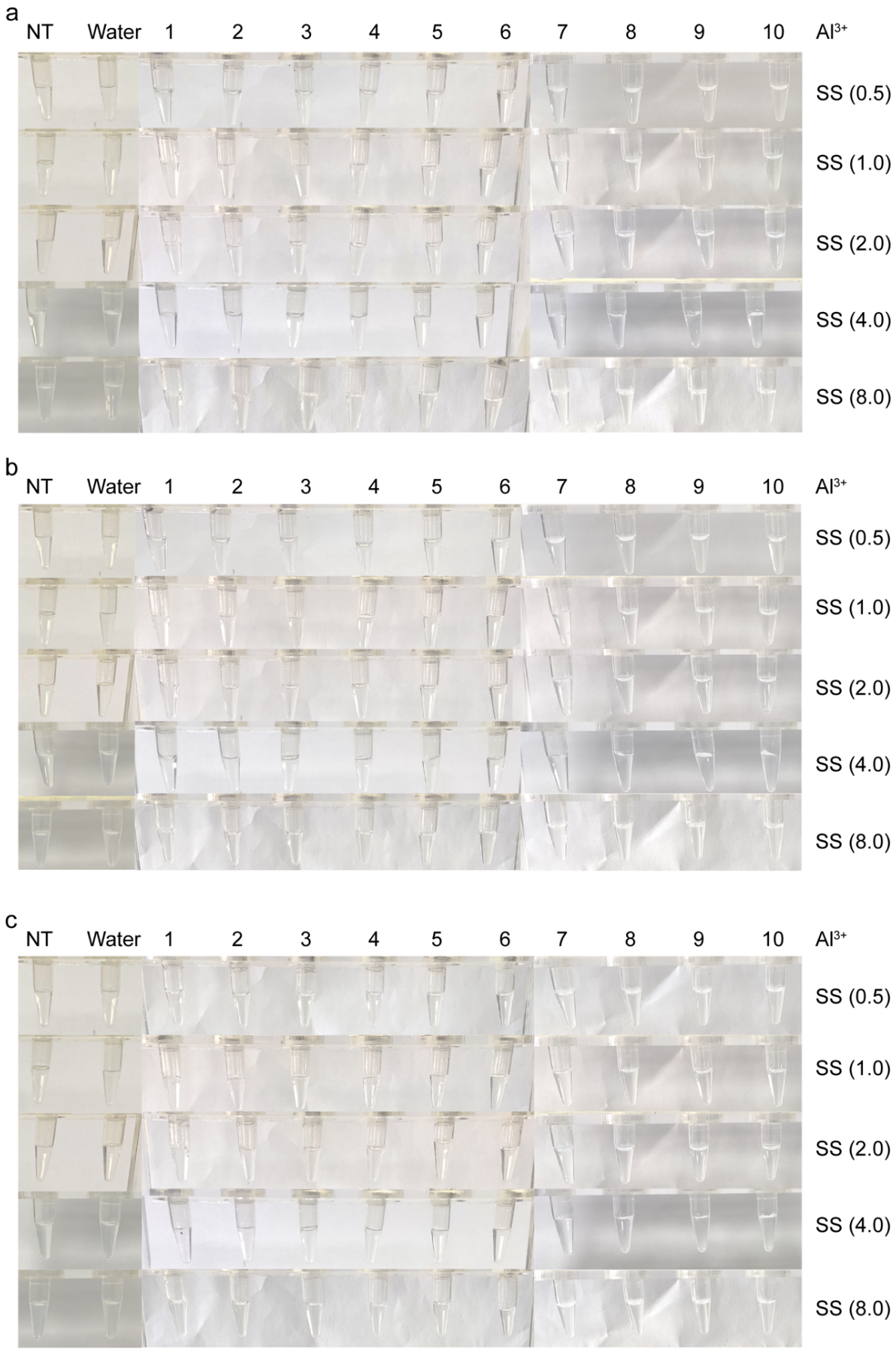

Fig. S8 Images of different concentrations of SS mixed with Al^{3+}.

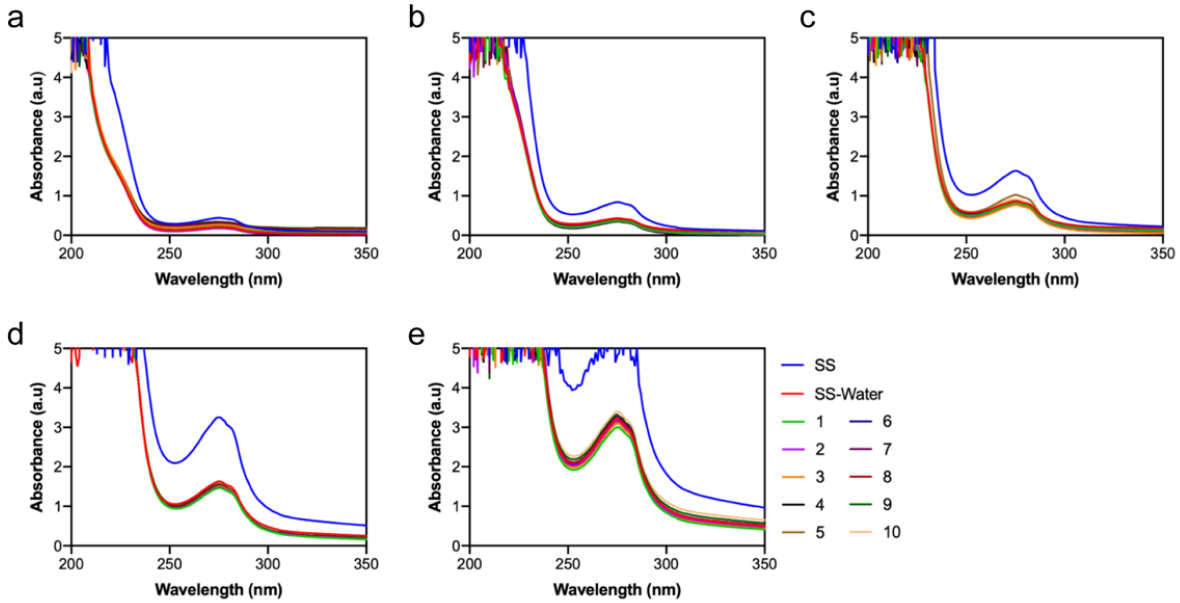

Fig. S9 UV-Vis absorbance of (a) SS (0.5), (b) SS (1.0), (c) SS (2.0), (d) SS (4.0), and (e) SS (8.0) mixed with Al^{3+} (Test 1).

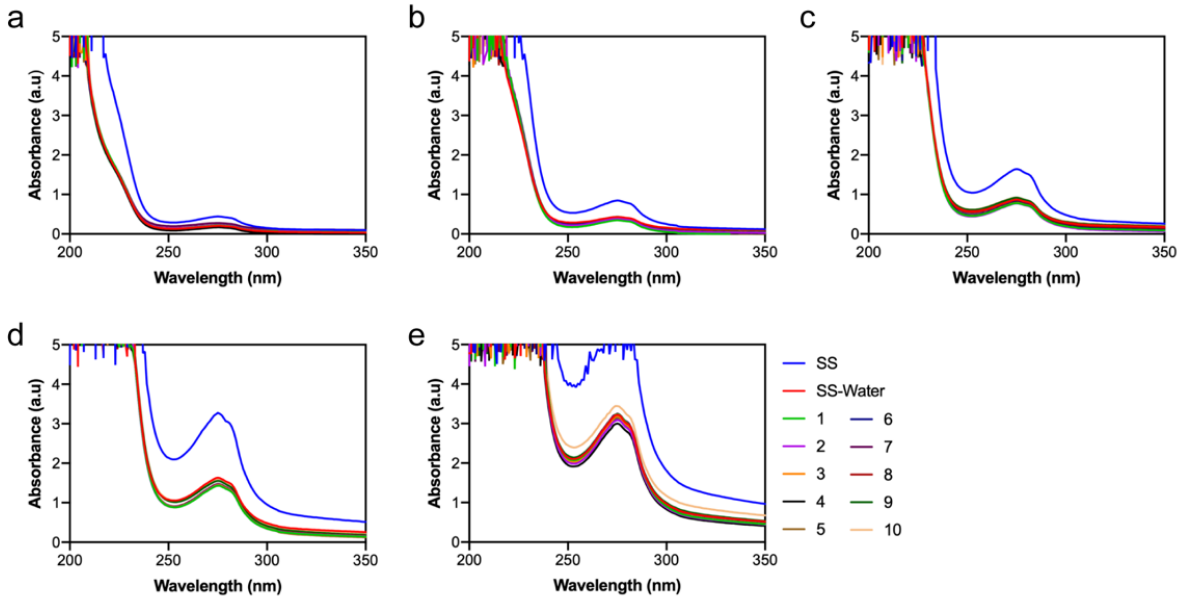

Fig. S10 UV-Vis absorbance of (a) SS (0.5), (b) SS (1.0), (c) SS (2.0), (d) SS (4.0), and (e) SS (8.0) mixed with Al^{3+} (Test 2).

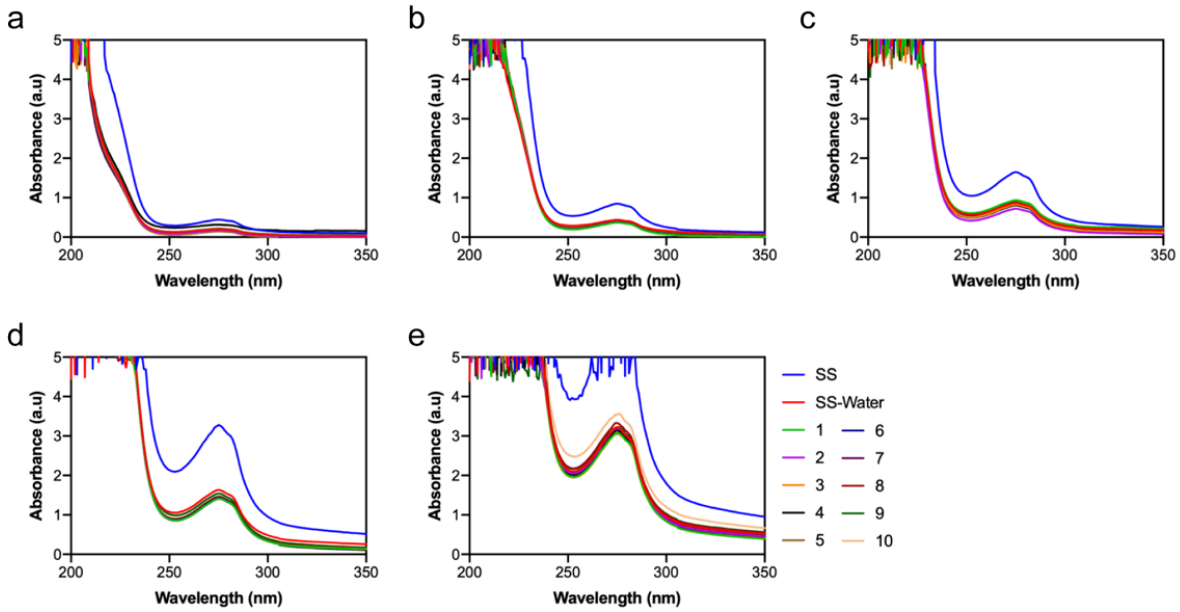

Fig. S11 UV-Vis absorbance of (a) SS (0.5), (b) SS (1.0), (c) SS (2.0), (d) SS (4.0), and (e) SS (8.0) mixed with Al^{3+} (Test 3).

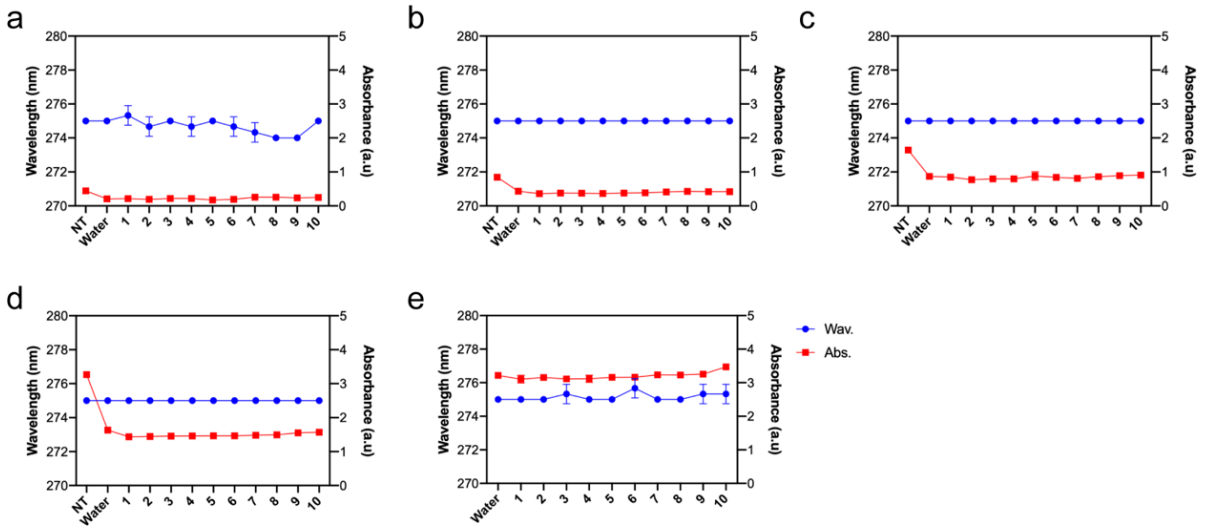

Fig. S12 UV-Vis absorbance change of (a) SS (0.5), (b) SS (1.0), (c) SS (2.0), (d) SS (4.0), and (e) SS (8.0) mixed with Al^{3+}.

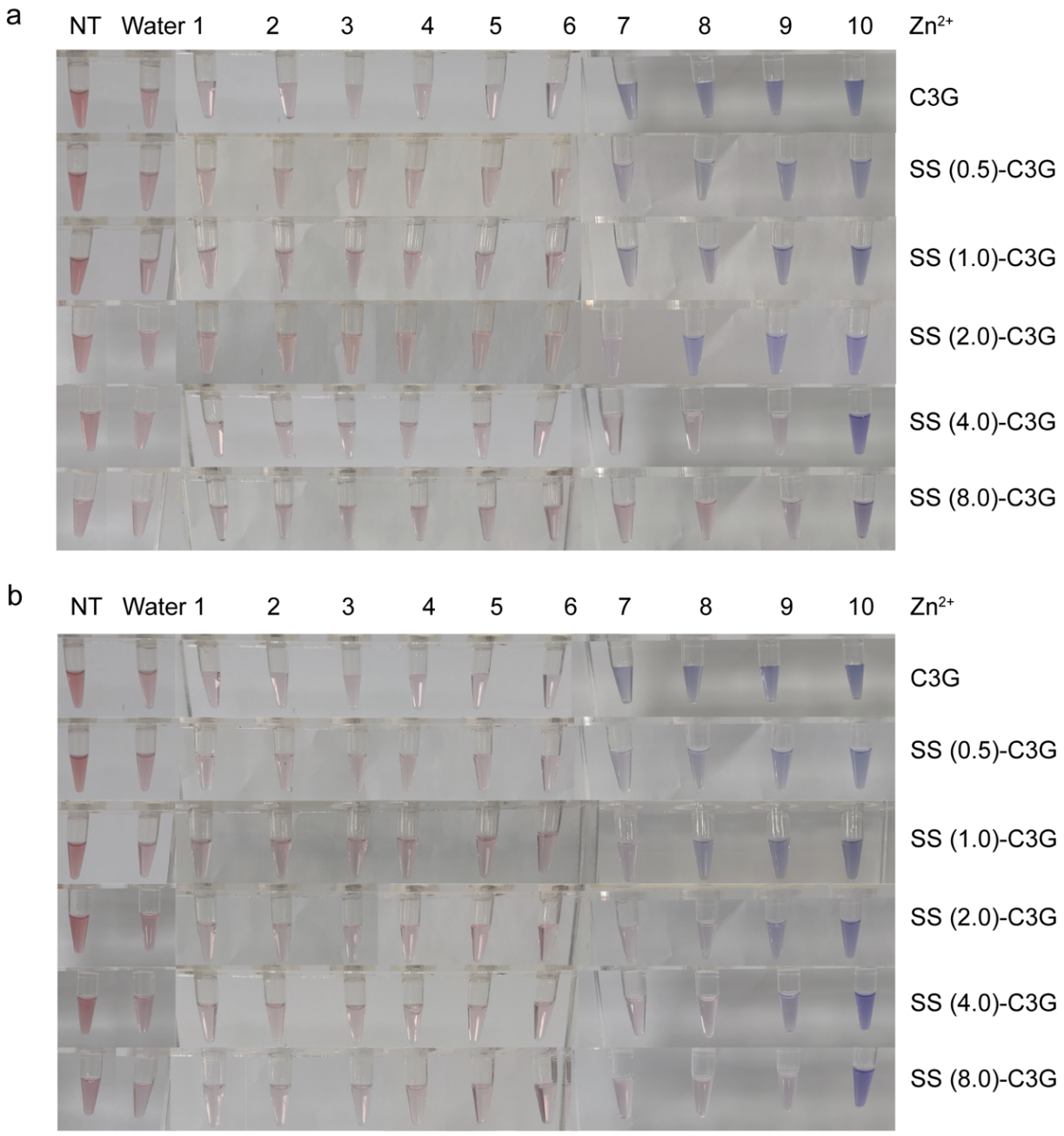

Fig. S13 Images of C3G and SS-C3G nanocomplex after mixing with different concentrations of Zn^{2+} (Repeated tests).

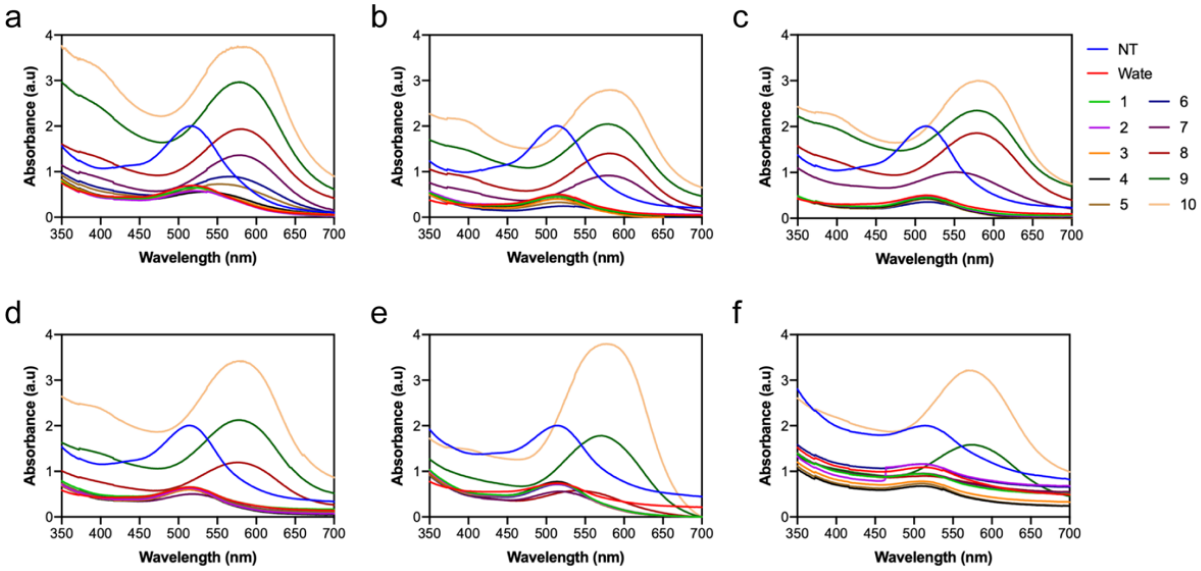

Fig. S14 UV-Vis absorbance (a) C3G, (b) SS (0.5)-C3G, (c) SS (1.0)-C3G, (d) SS (2.0)-C3G, (e) SS (4.0)-C3G, and (f) SS (8.0)-C3G mixed with different concentrations of Zn^{2+} (Test 1).

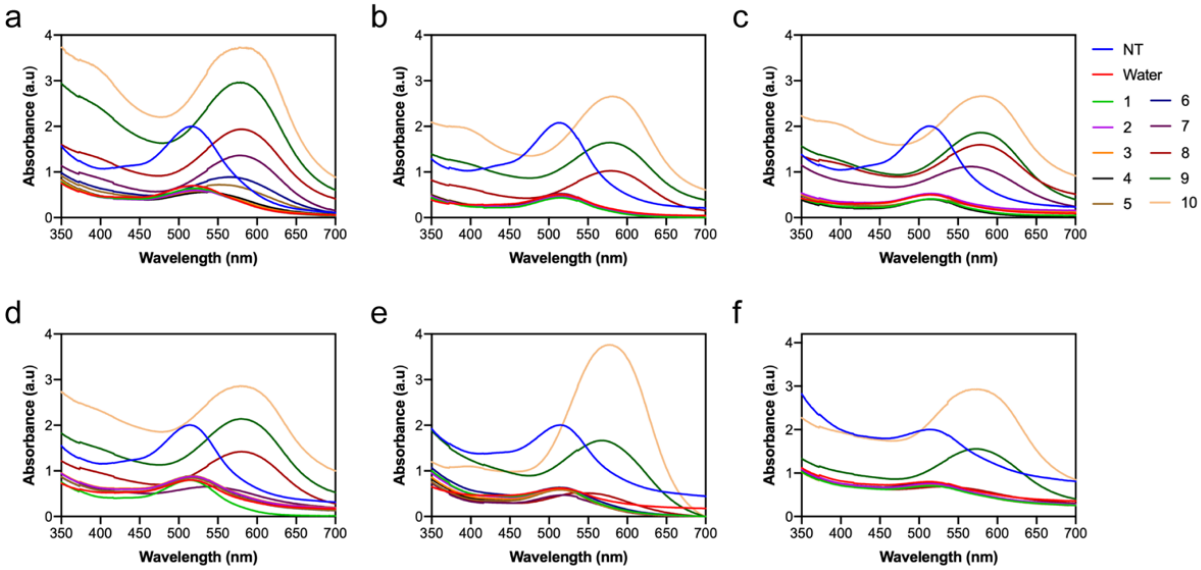

Fig. S15 UV-Vis absorbance (a) C3G, (b) SS (0.5)-C3G, (c) SS (1.0)-C3G, (d) SS (2.0)-C3G, (e) SS (4.0)-C3G, and (f) SS (8.0)-C3G mixed with different concentrations of Zn^{2+} (Test 2).

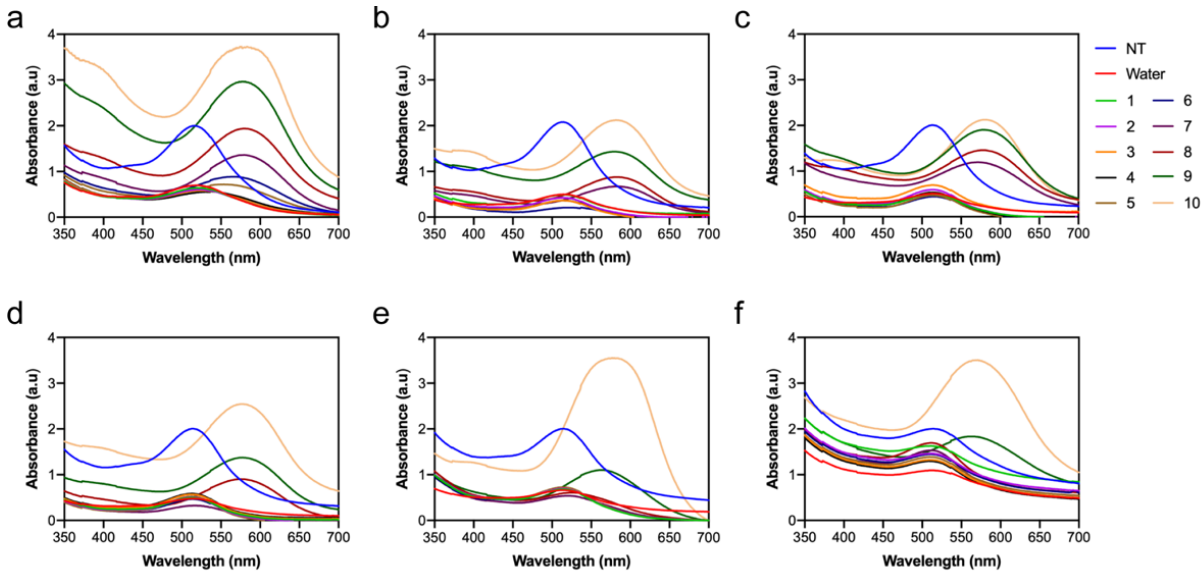

Fig. S16 UV-Vis absorbance (a) C3G, (b) SS (0.5)-C3G, (c) SS (1.0)-C3G, (d) SS (2.0)-C3G, (e) SS (4.0)-C3G, and (f) SS (8.0)-C3G mixed with different concentrations of Zn^{2+} (Test 3).

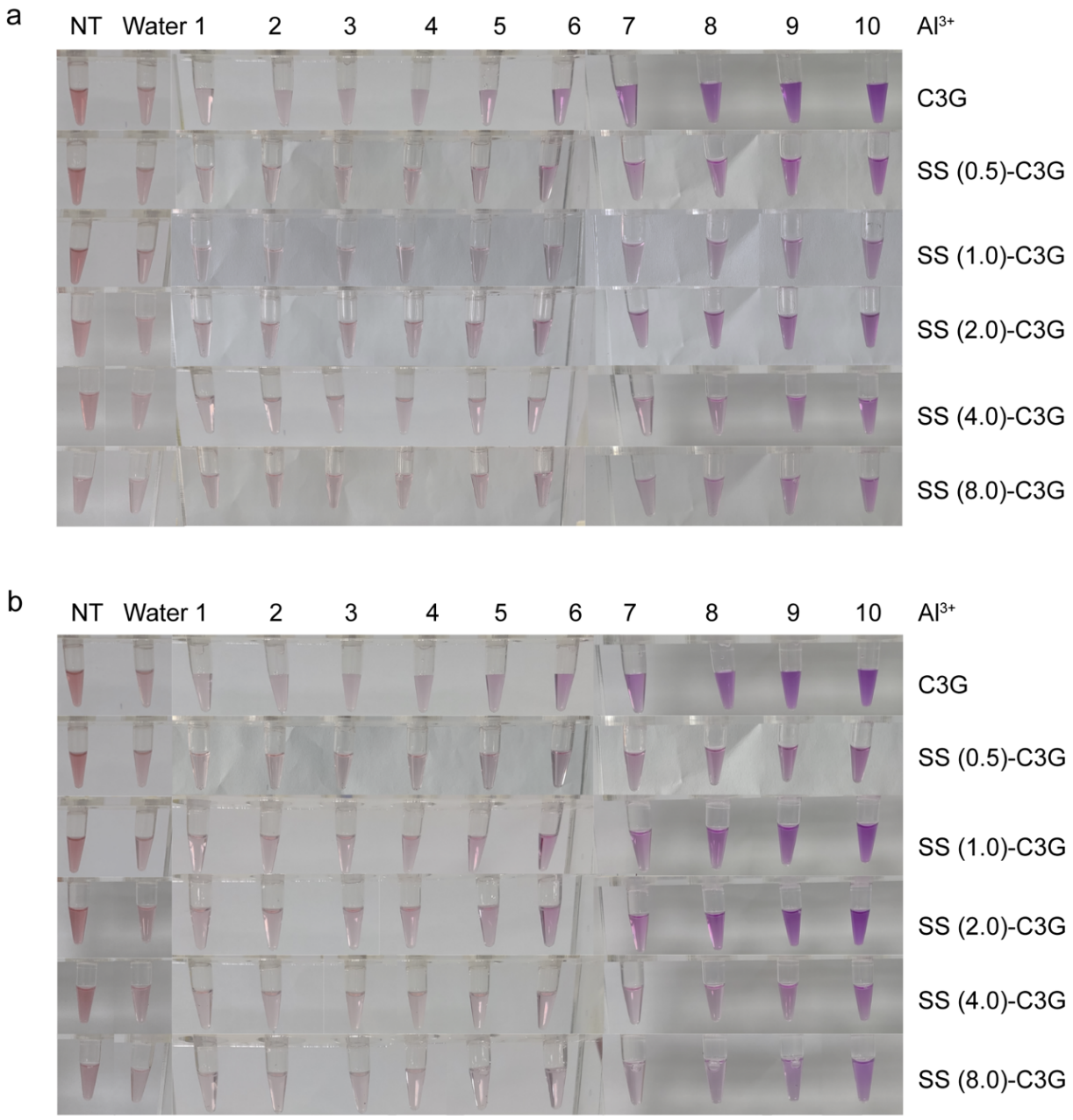

Fig. S17 Images of C3G and SS-C3G nanocomplex after mixing with different concentrations of Al^{3+} (Repeated tests).

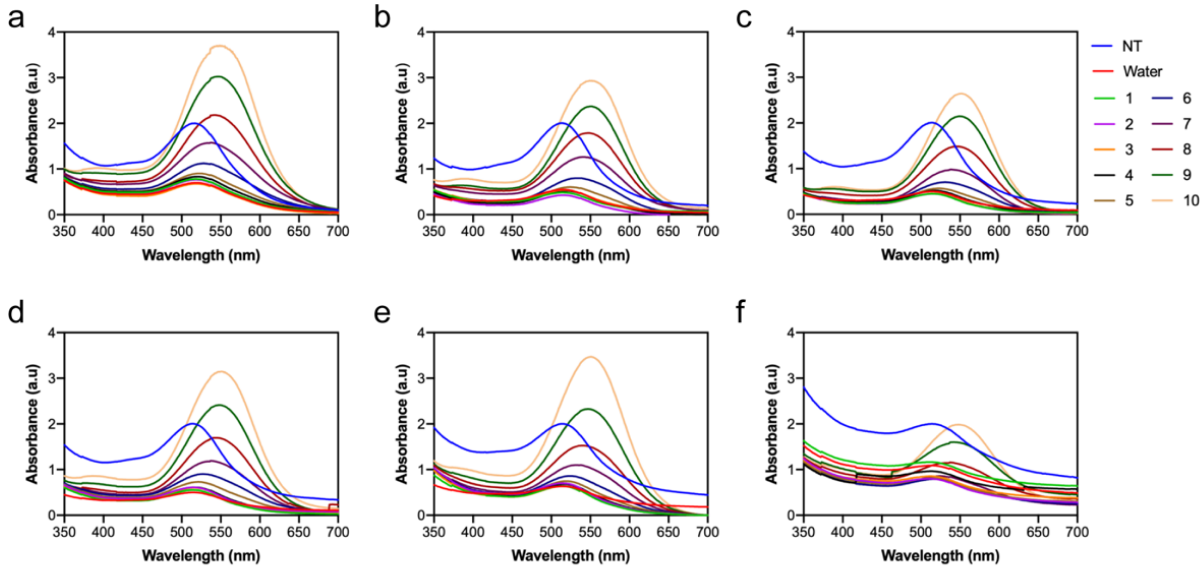

Fig. S18 UV-Vis absorbance (a) C3G, (b) SS (0.5)-C3G, (c) SS (1.0)-C3G, (d) SS (2.0)-C3G, (e) SS (4.0)-C3G, and (f) SS (8.0)-C3G mixed with different concentrations of Al^{3+} (Test 1).

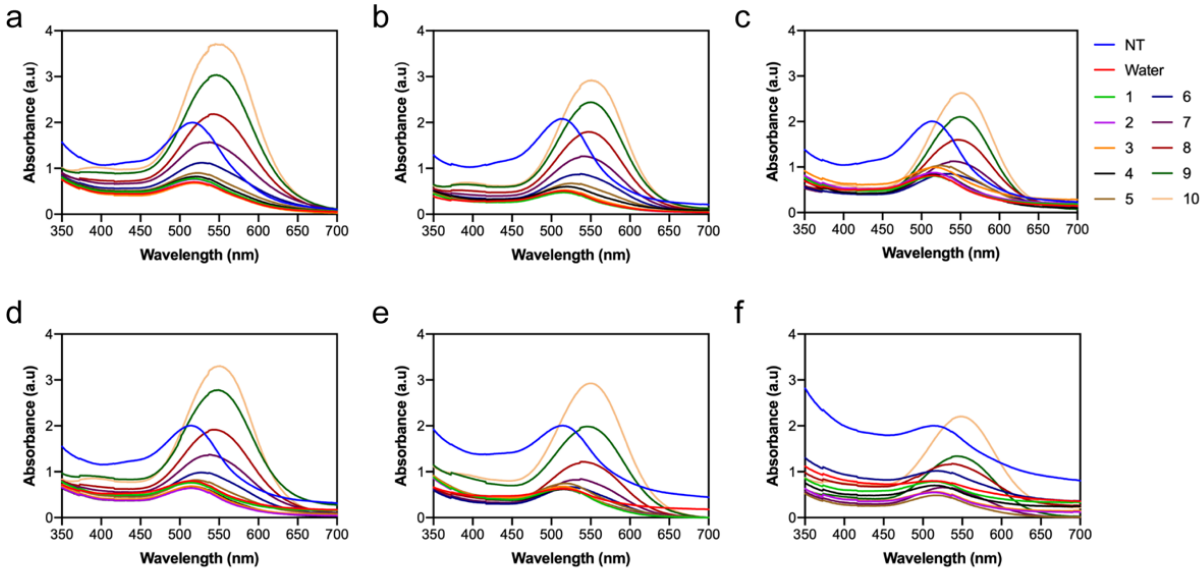

Fig. S19 UV-Vis absorbance (a) C3G, (b) SS (0.5)-C3G, (c) SS (1.0)-C3G, (d) SS (2.0)-C3G, (e) SS (4.0)-C3G, and (f) SS (8.0)-C3G mixed with different concentrations of Al^{3+} (Test 2).

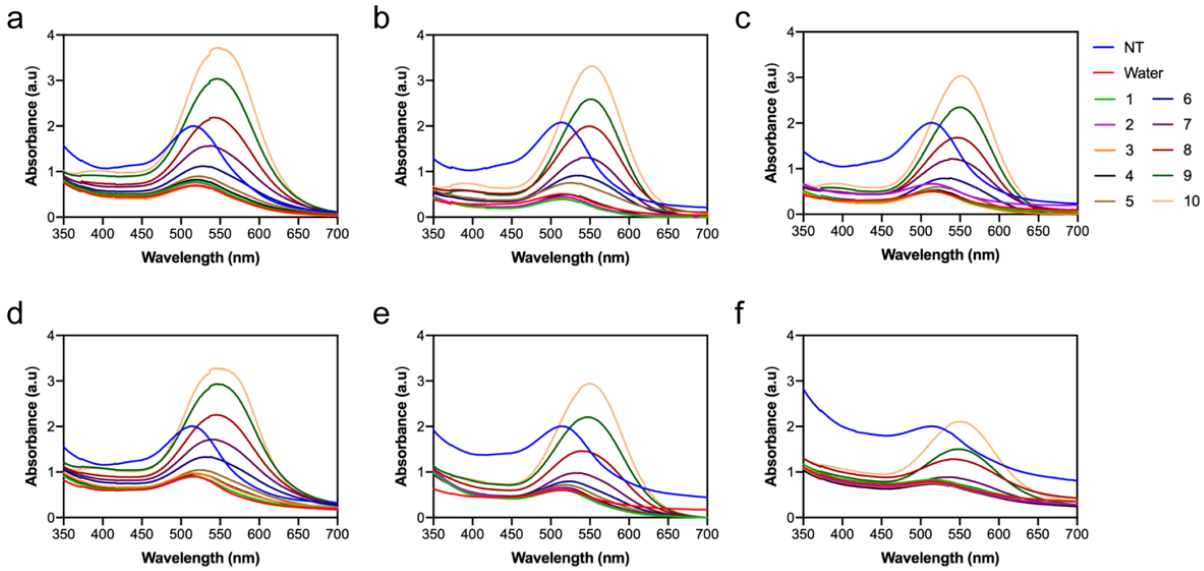

Fig. S20 UV-Vis absorbance (a) C3G, (b) SS (0.5)-C3G, (c) SS (1.0)-C3G, (d) SS (2.0)-C3G, (e) SS (4.0)-C3G, and (f) SS (8.0)-C3G mixed with different concentrations of Al^{3+} (Test 3).

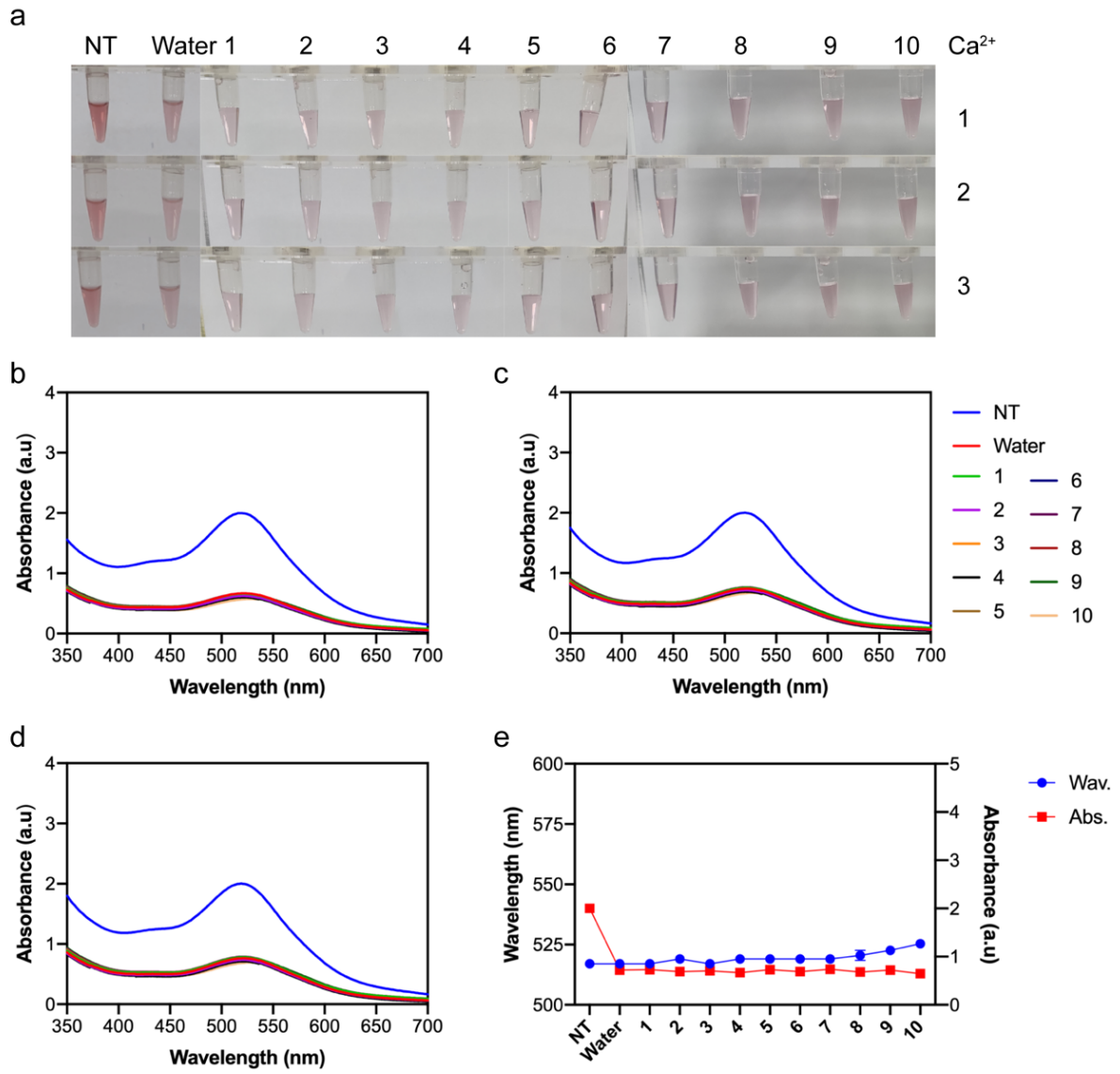

Fig. S21 (a) Images of C3G mixed with Ca^{2+}. (b-c) UV-Vis absorbance and (e) UV-Vis absorbance change of C3G mixed with Ca^{2+}.

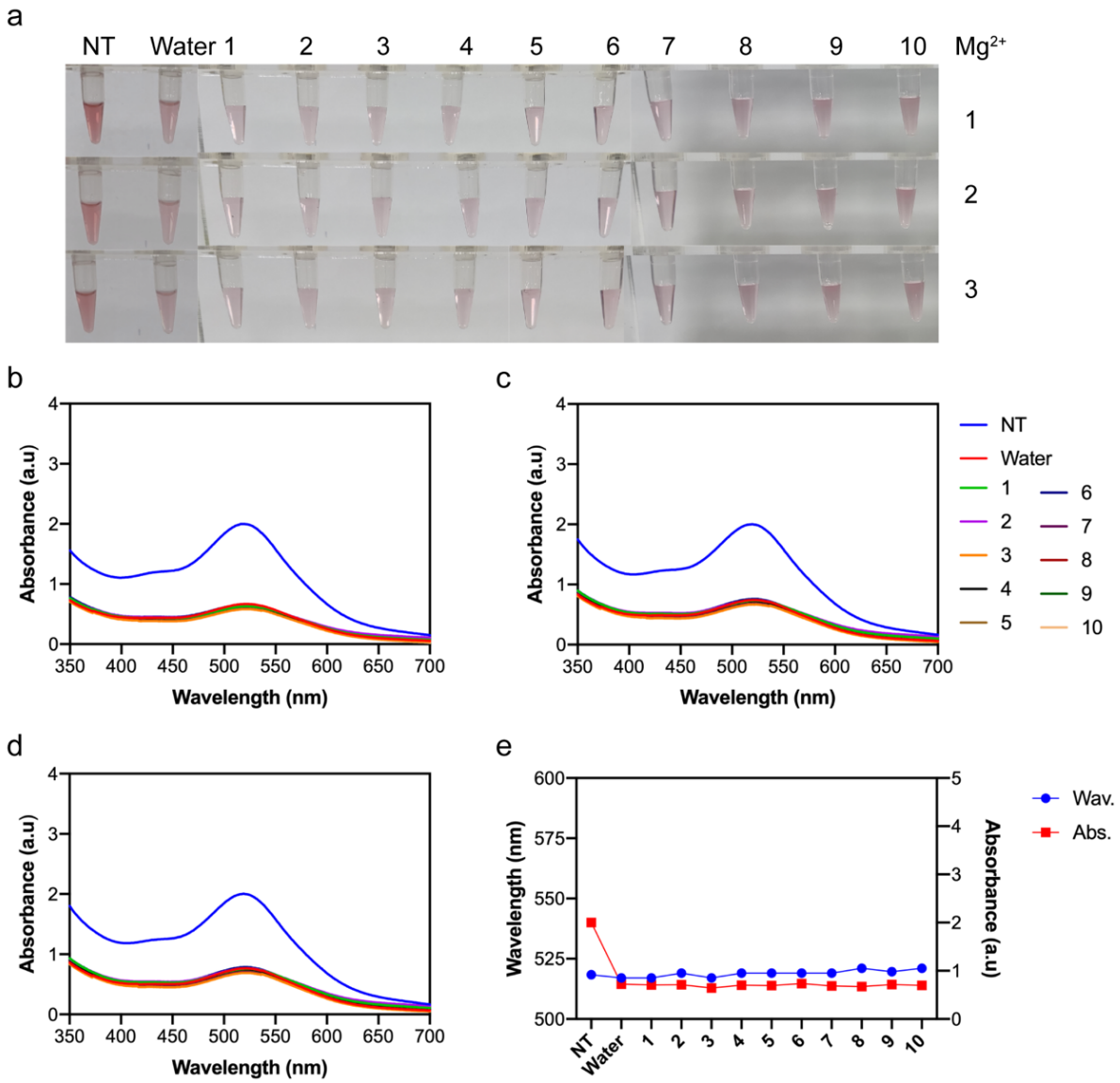

Fig. S22 (a) Images of C3G mixed with Mg^{2+}. (b-c) UV-Vis absorbance and (e) UV-Vis absorbance change of C3G mixed with Mg^{2+}.

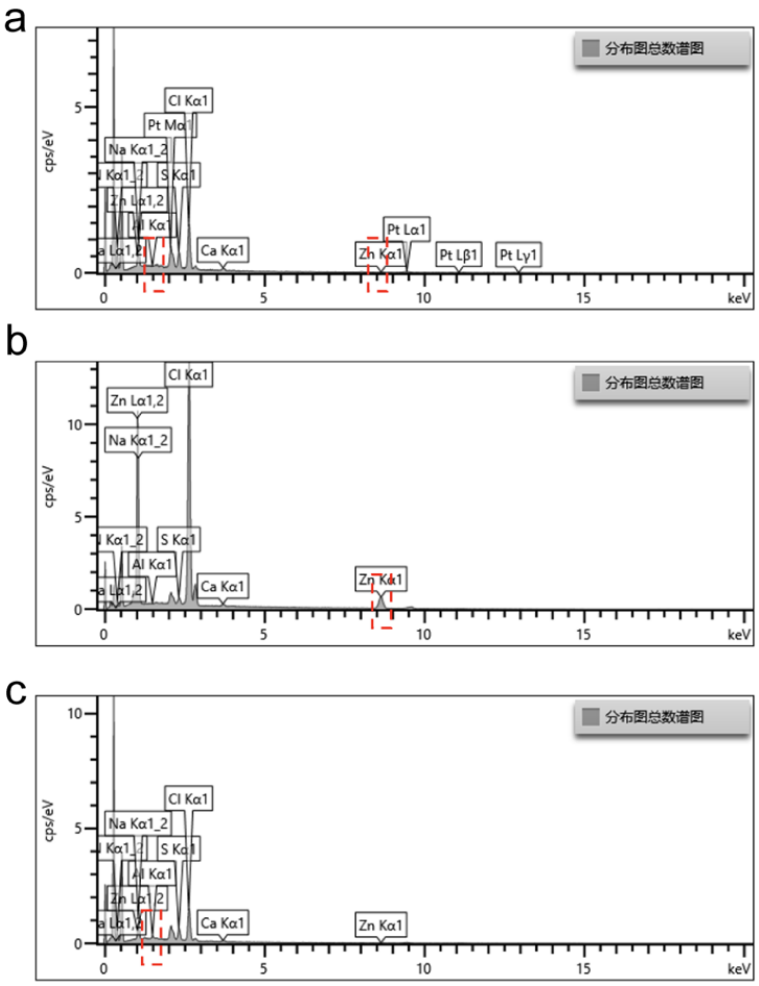

Fig. S23 EDS result of (a) SS (4.0)-C3G, (b) SS (4.0)-C3G-Zn-10, (c) SS (4.0)-C3G-Al-10.

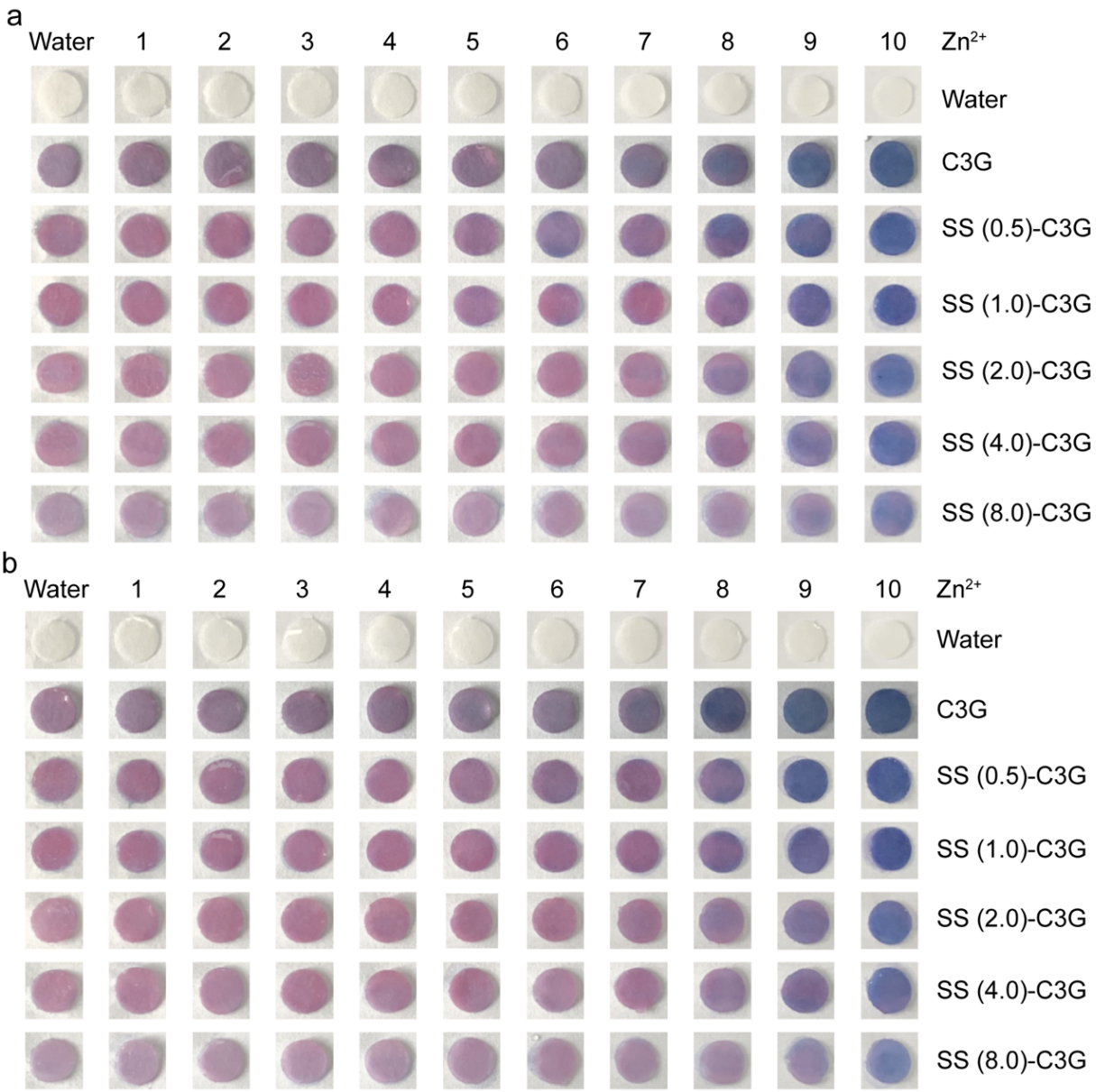

Fig. S24 Images of C3G and SS-C3G nanocomplex films (filter paper) after mixing with different concentrations of Zn^{2+} (Repeated tests).

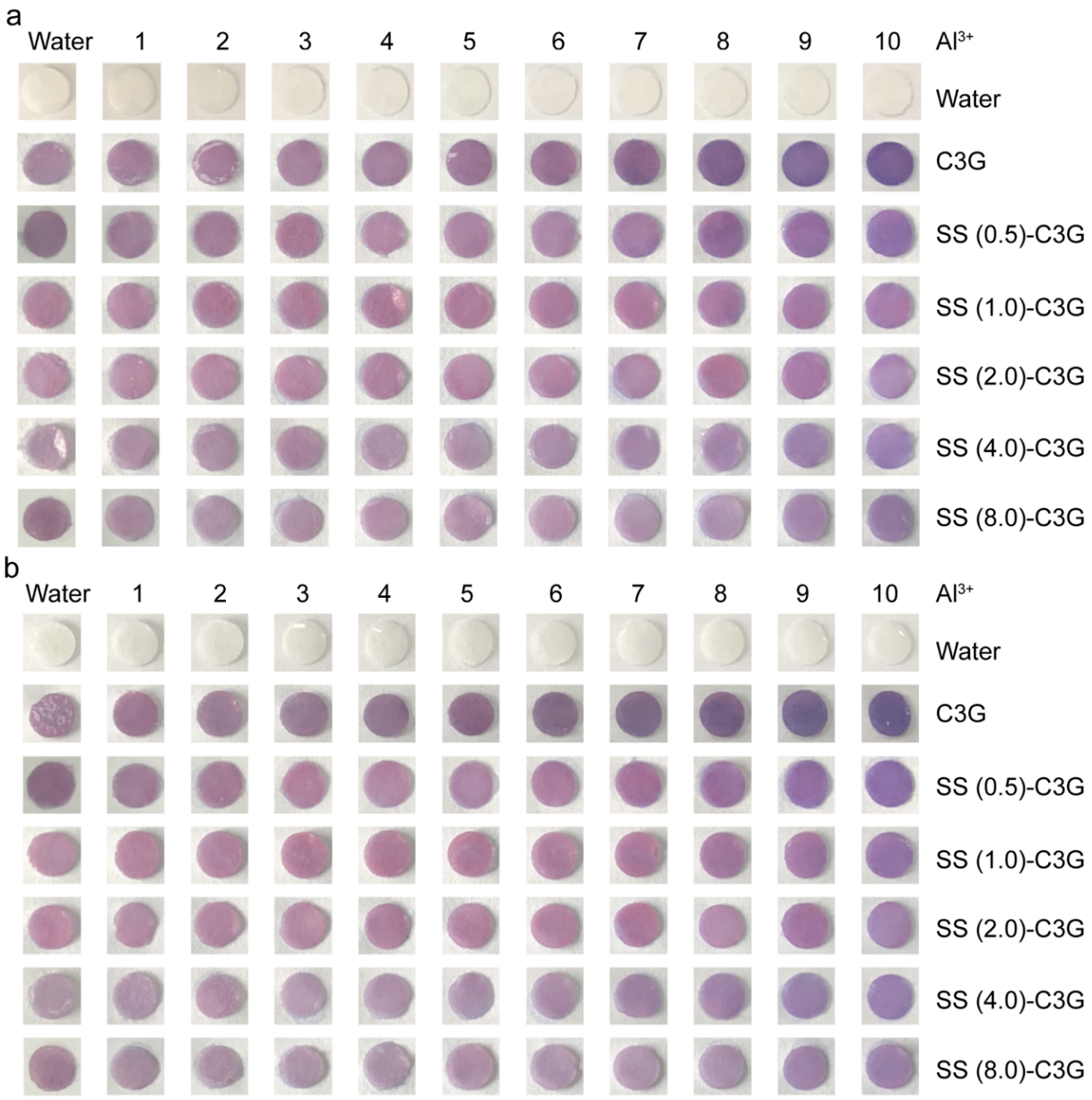

Fig. S25 Images of C3G and SS-C3G nanocomplex films (filter paper) after mixing with different concentrations of Al^{3+} (Repeated tests).

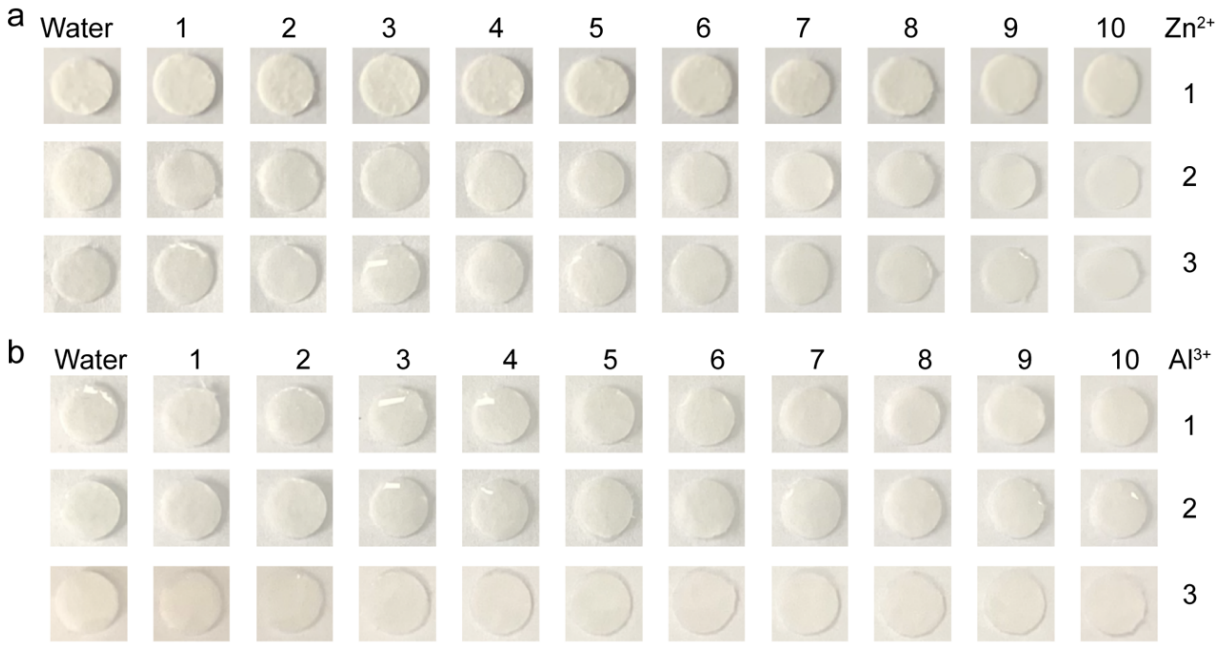

Fig. S26 Images of filter paper after mixing with different concentrations of (a) Zn^{2+} and (b) Al^{3+}.

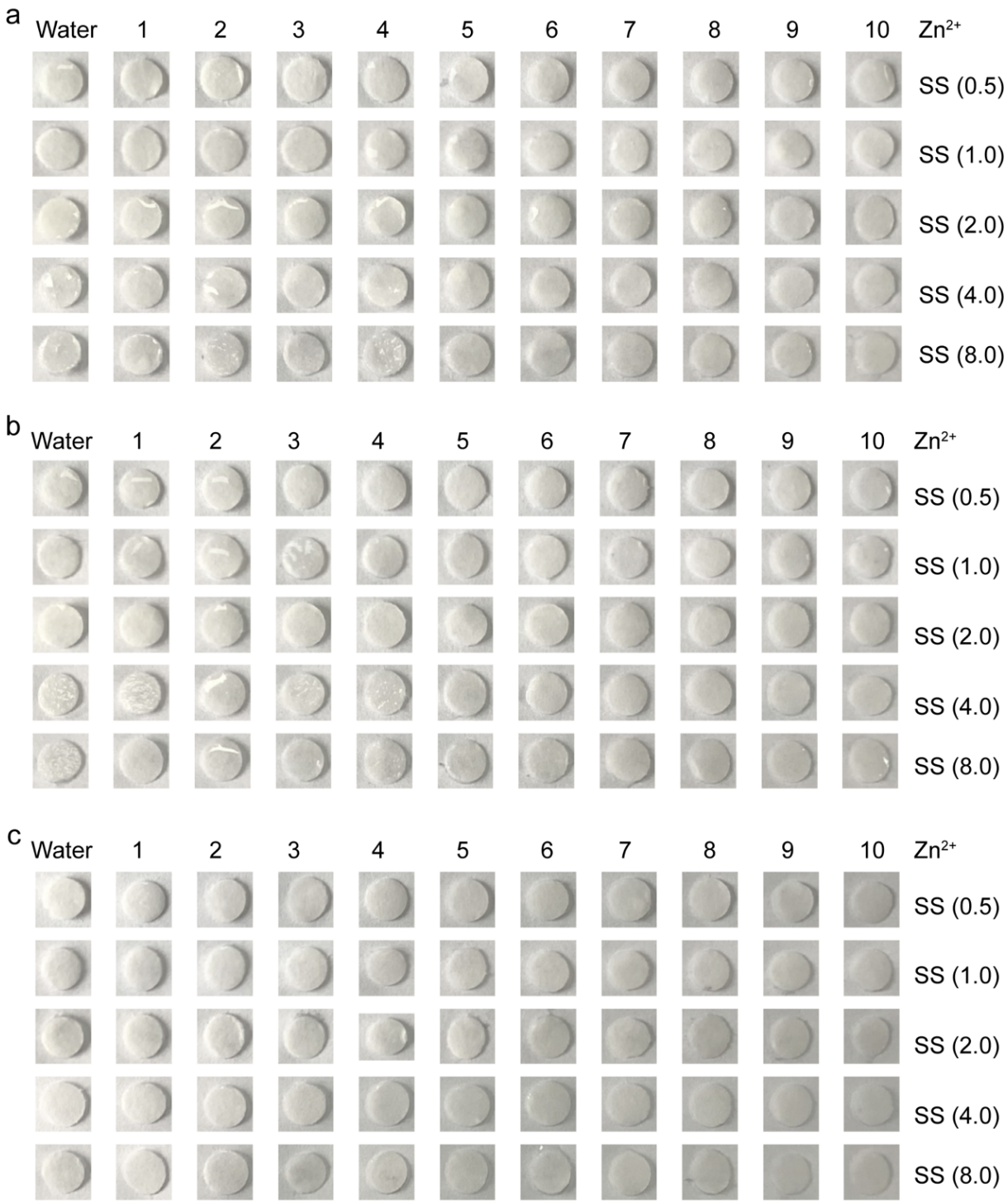

Fig. S27 Images of SS films (filter paper) after mixing with different concentrations of Zn^{2+}. (Repeated tests).

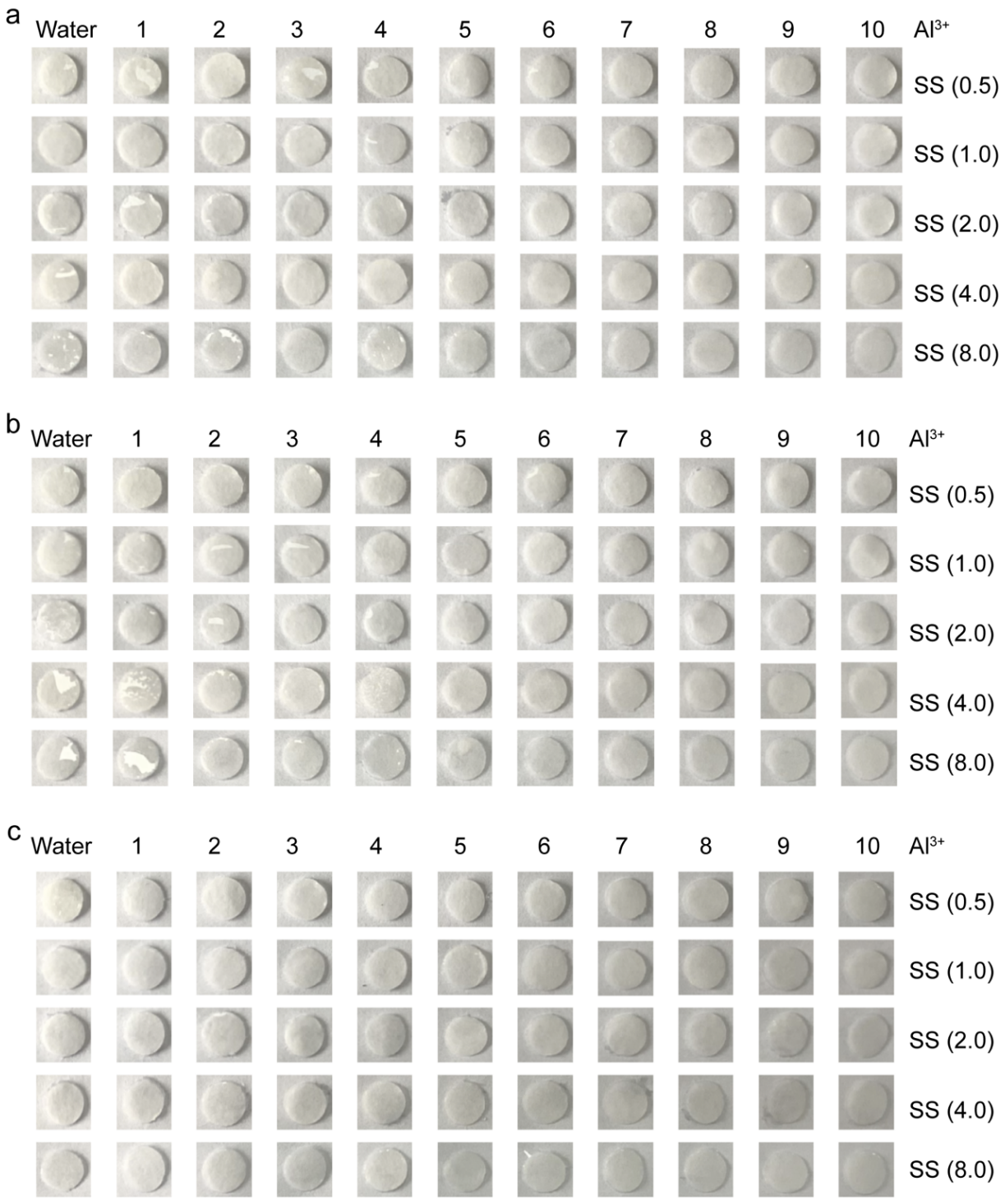

Fig. S28 Images of SS films (filter paper) after mixing with different concentrations of Al^{3+}. (Repeated tests).

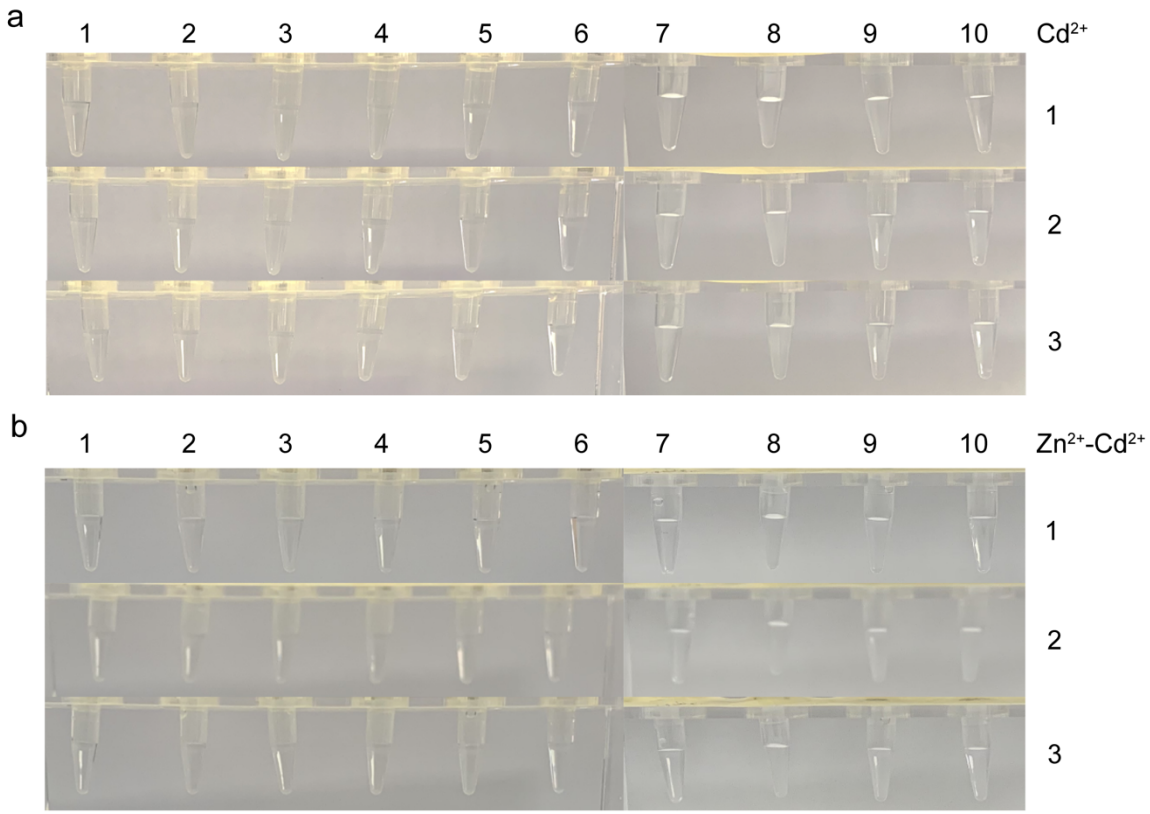

Fig. S29 Images of different concentrations of (a) Cd^{2+} and (b) Zn^{2+}-Cd^{2+} solutions.

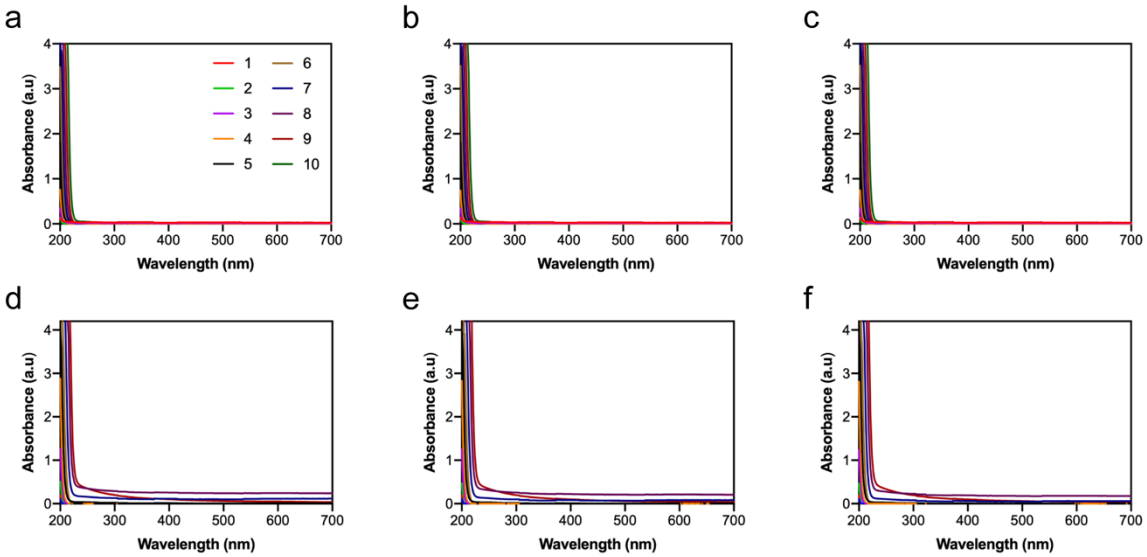

Fig. S30 UV-Vis absorbance of different concentrations of (a-c) Cd^{2+} and (d-f) Zn^{2+}, (g-i) Zn^{2+}-Cd^{2+}.

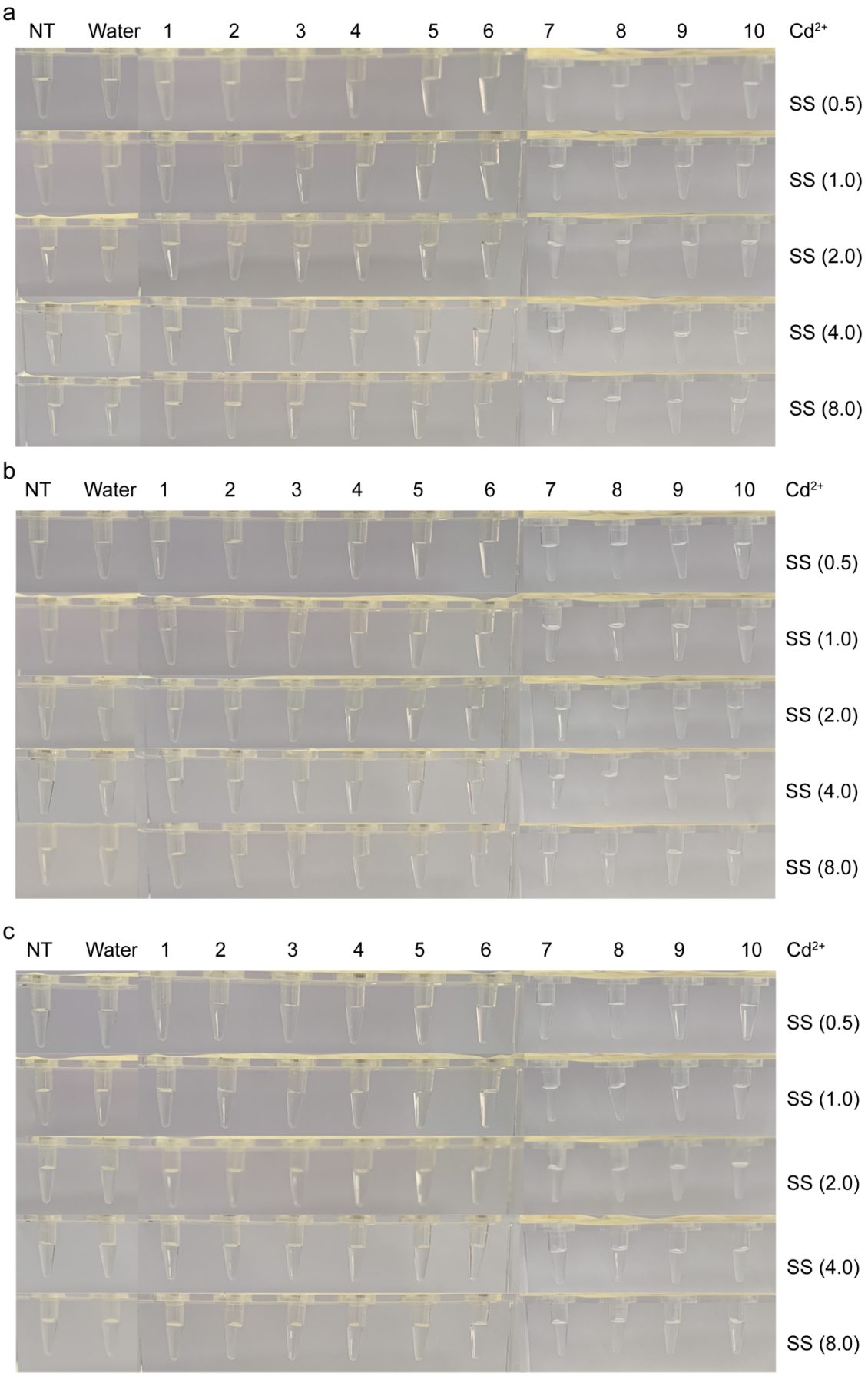

Fig. S31 Images of different concentrations of SS mixed with Cd^{2+}.

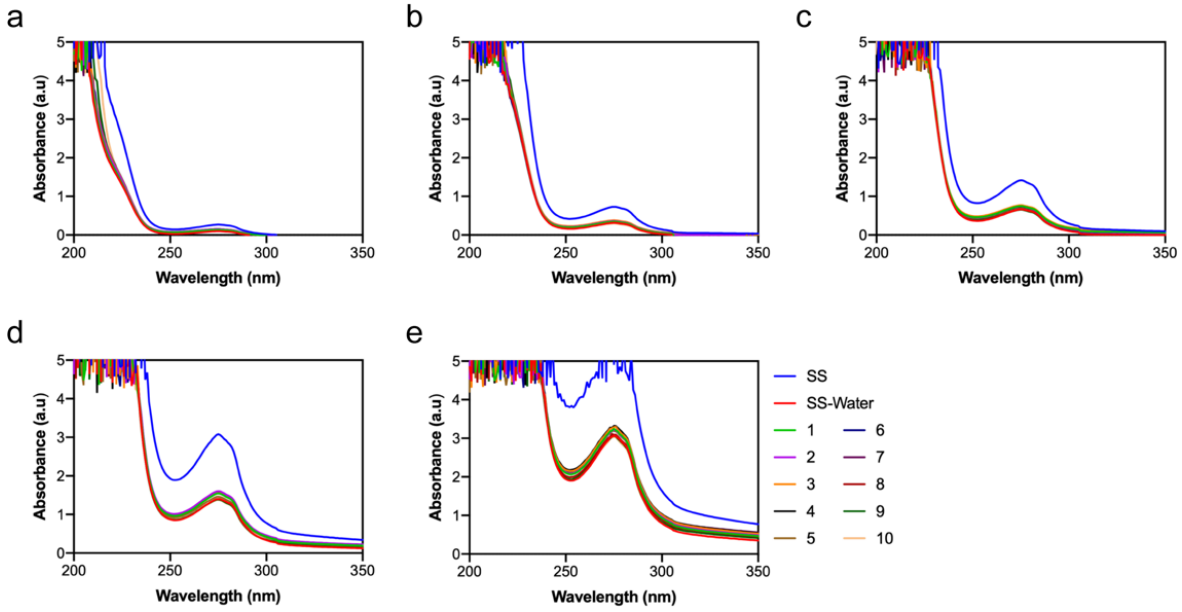

Fig. S32 UV-Vis absorbance of (a) SS (0.5), (b) SS (1.0), (c) SS (2.0), (d) SS (4.0), and (e) SS (8.0) mixed with Cd^{2+} (Test 1).

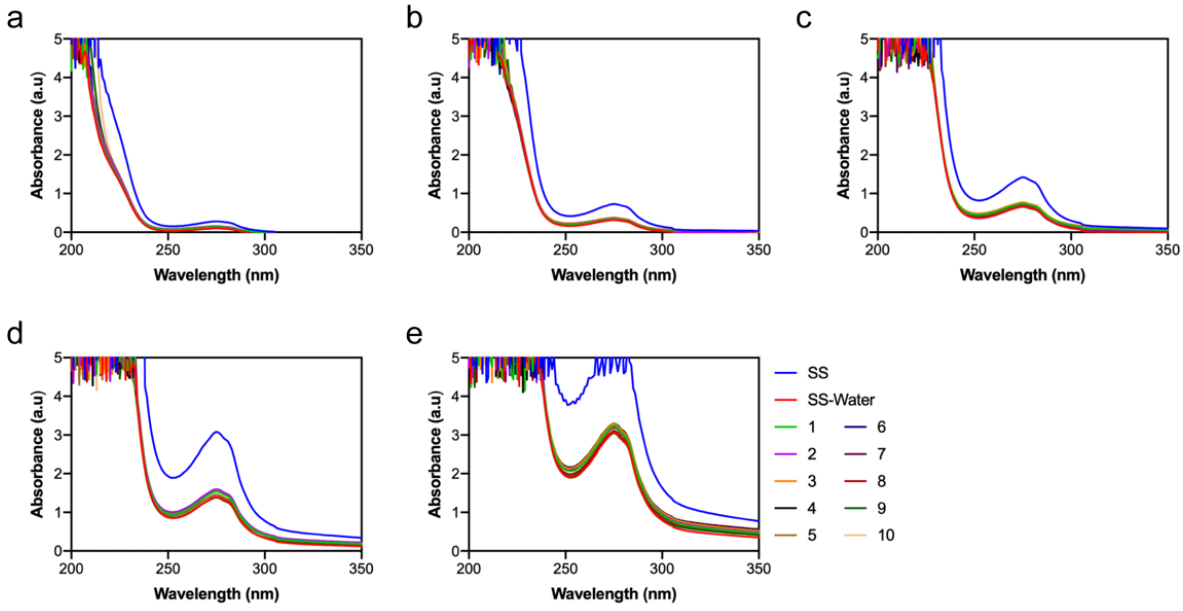

Fig. S33 UV-Vis absorbance of (a) SS (0.5), (b) SS (1.0), (c) SS (2.0), (d) SS (4.0), and (e) SS (8.0) mixed with Cd^{2+} (Test 2).

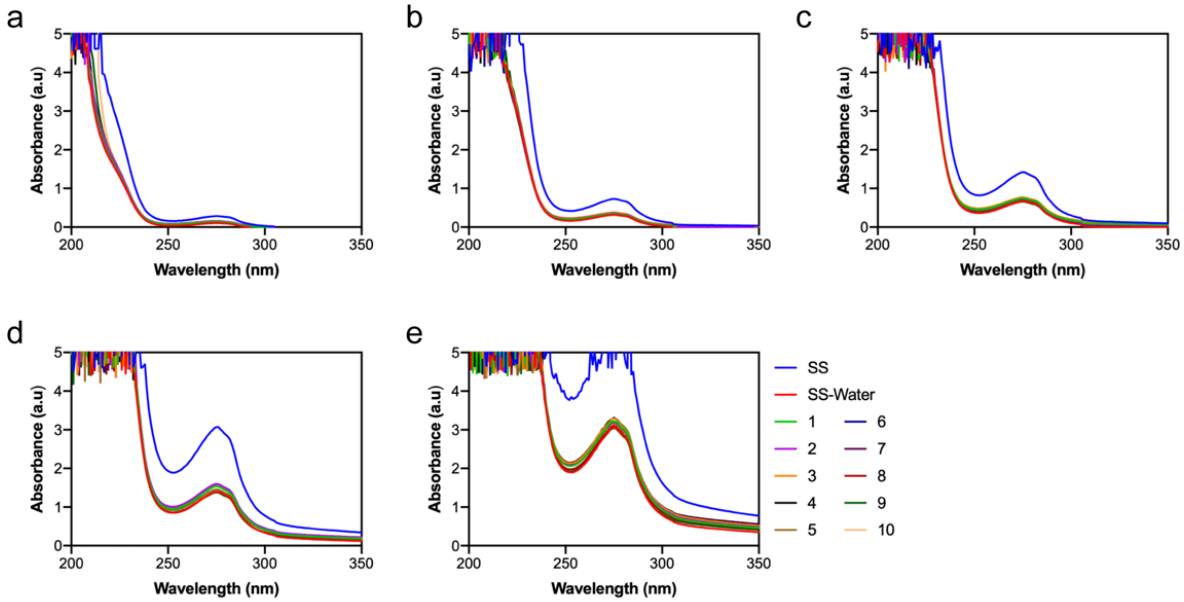

Fig. S34 UV-Vis absorbance of (a) SS (0.5), (b) SS (1.0), (c) SS (2.0), (d) SS (4.0), and (e) SS (8.0) mixed with Cd^{2+} (Test 3).

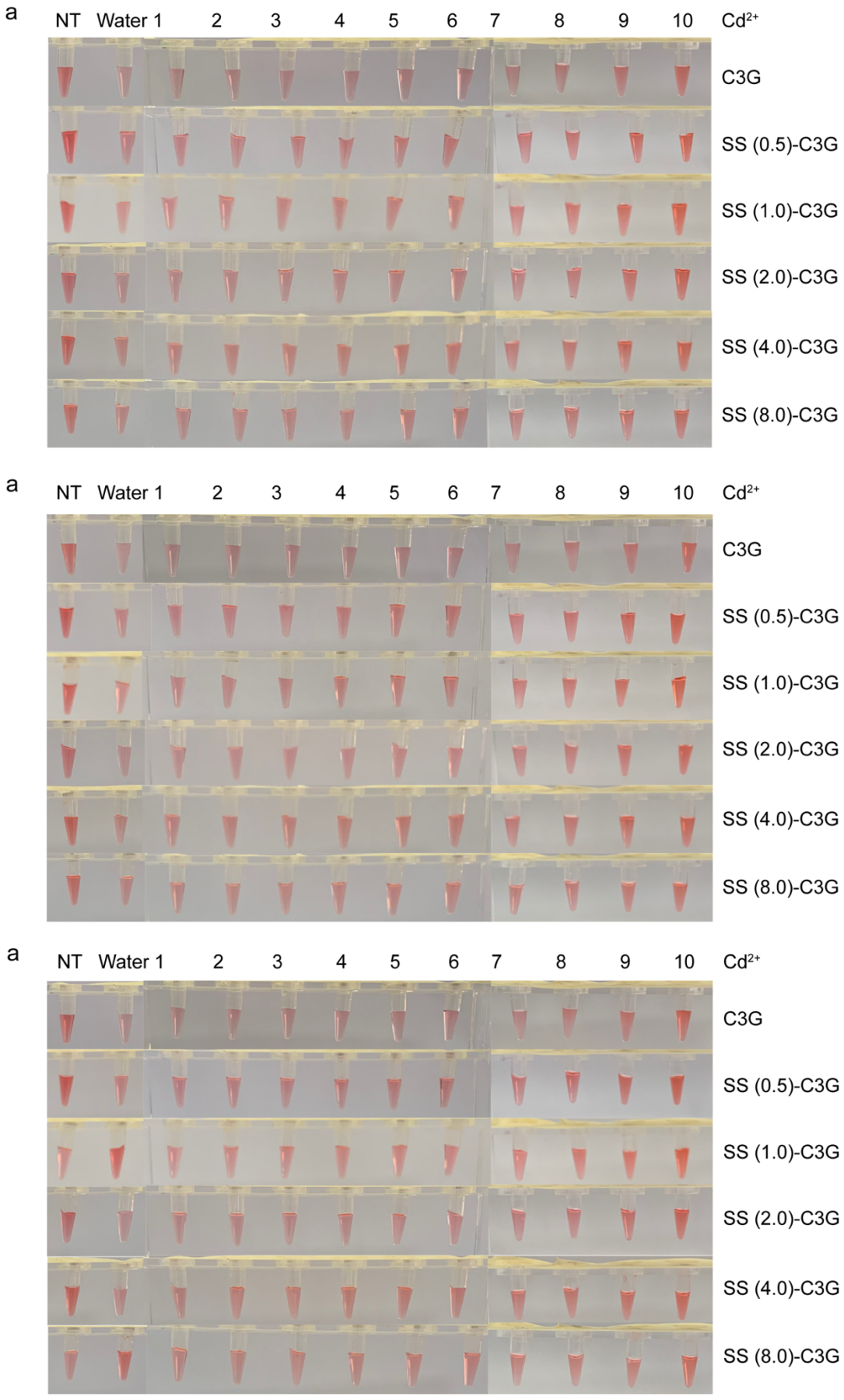

Fig. S35 Images of C3G and SS-C3G nanocomplex after mixing with different concentrations of Cd^{2+}.

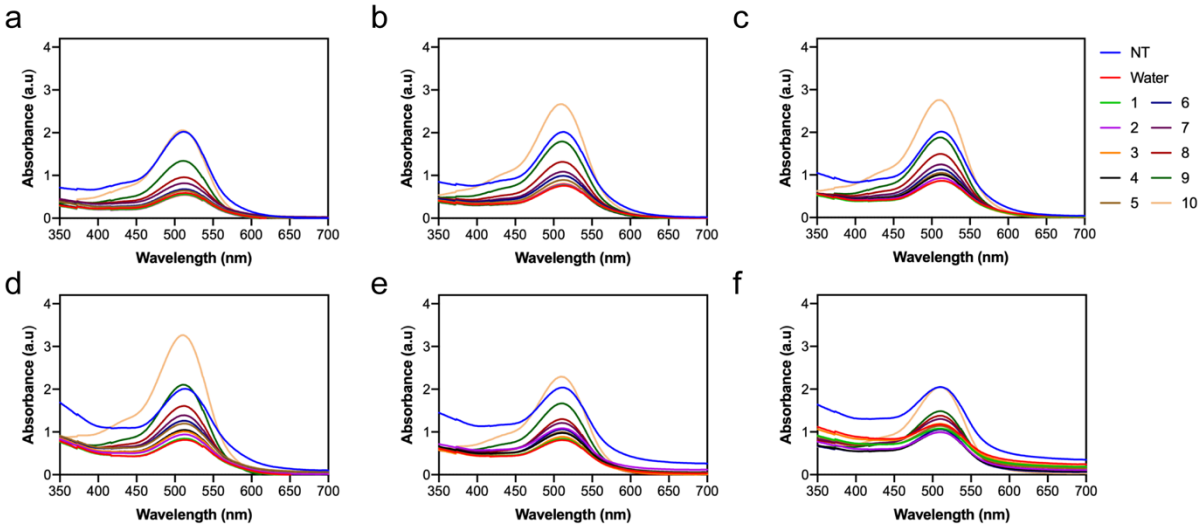

Fig. S36 UV-Vis absorbance (a) C3G, (b) SS (0.5)-C3G, (c) SS (1.0)-C3G, (d) SS (2.0)-C3G, (e) SS (4.0)-C3G, and (f) SS (8.0)-C3G mixed with different concentrations of Cd^{2+} (Test 1).

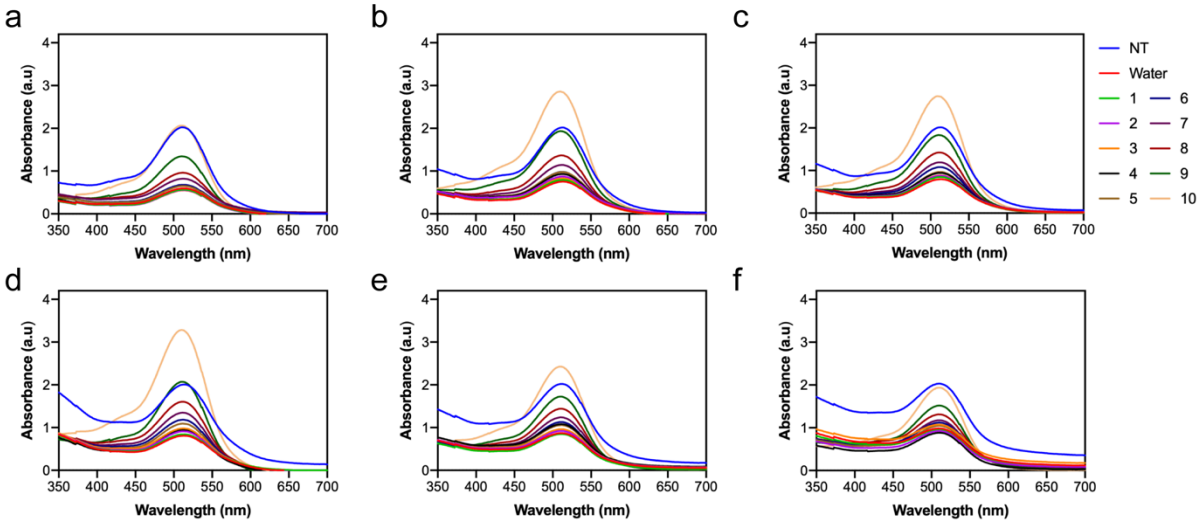

Fig. S37 UV-Vis absorbance (a) C3G, (b) SS (0.5)-C3G, (c) SS (1.0)-C3G, (d) SS (2.0)-C3G, (e) SS (4.0)-C3G, and (f) SS (8.0)-C3G mixed with different concentrations of Cd^{2+} (Test 2).

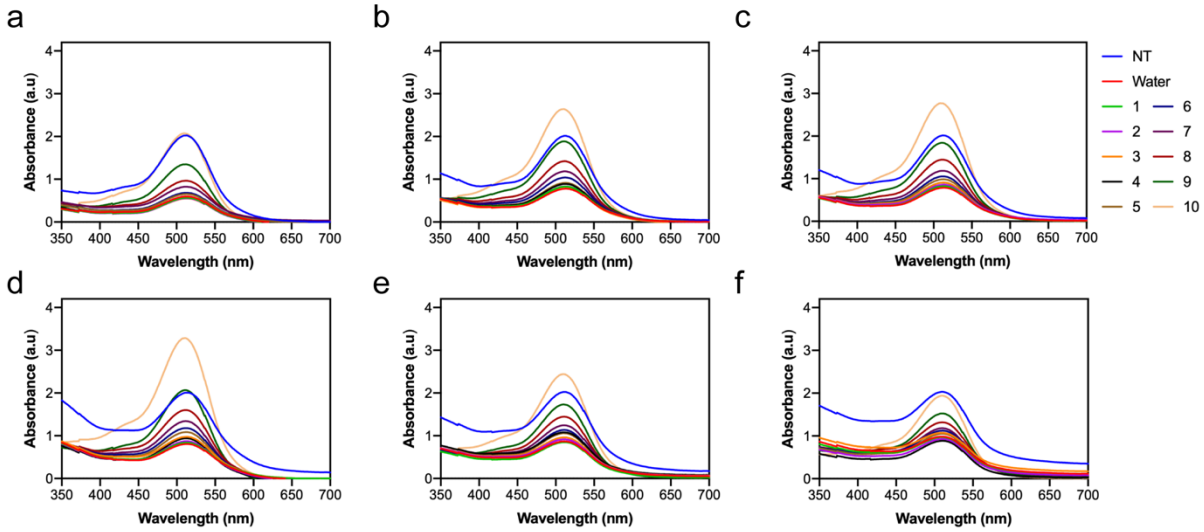

Fig. S38 UV-Vis absorbance (a) C3G, (b) SS (0.5)-C3G, (c) SS (1.0)-C3G, (d) SS (2.0)-C3G, (e) SS (4.0)-C3G, and (f) SS (8.0)-C3G mixed with different concentrations of Cd^{2+} (Test 3).

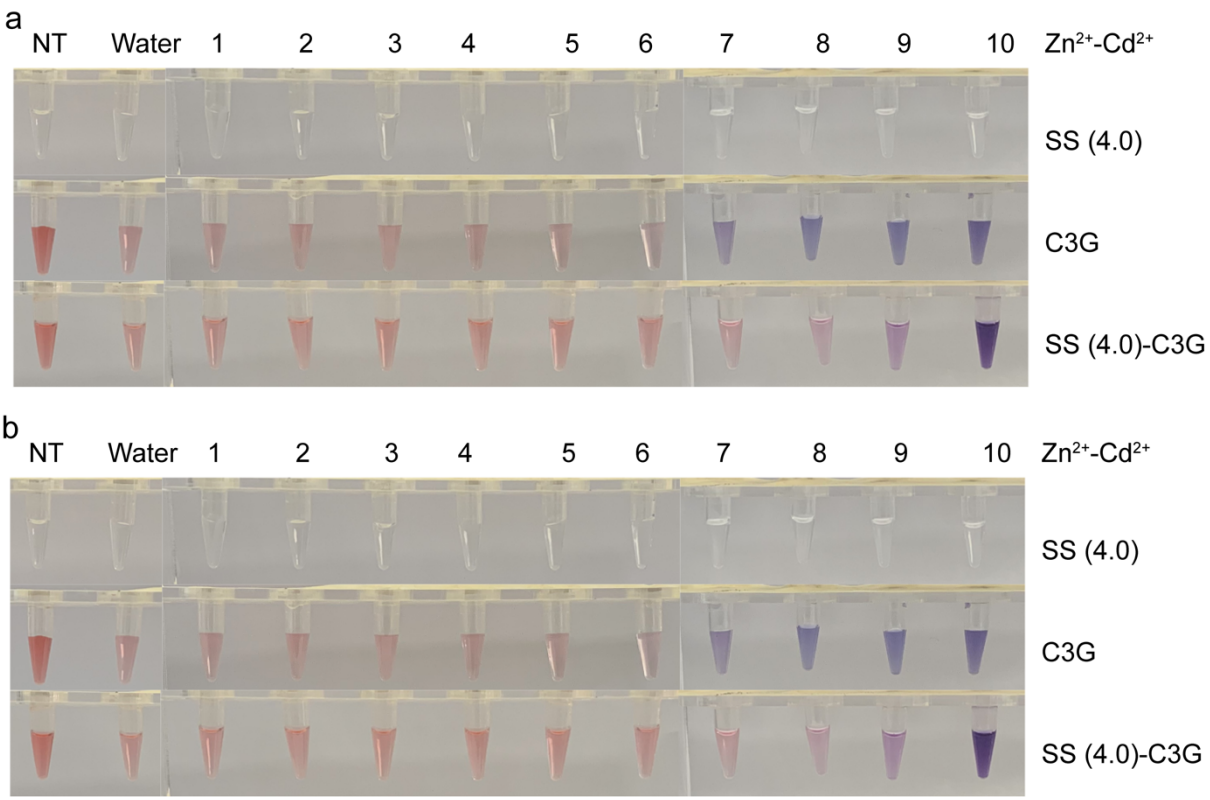

Fig. S39 Images of C3G and SS-C3G nanocomplex after mixing with different concentrations of Zn^{2+}-Cd^{2+}.

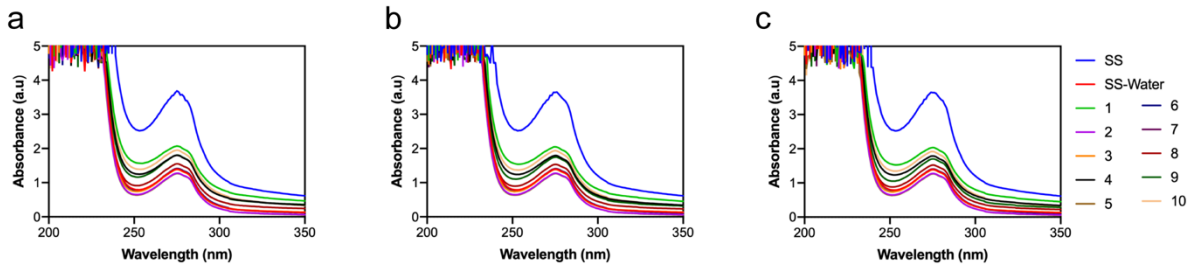

Fig. S40 UV-Vis absorbance SS (4.0) mixed with different concentrations of Zn^{2+}-Cd^{2+}.

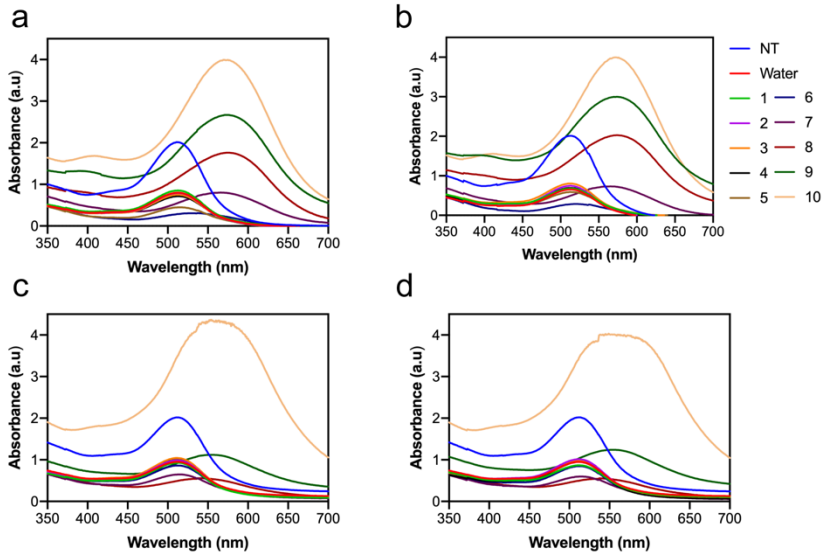

Fig. S41 UV-Vis absorbance (a-b) C3G and (c-d) SS (4.0)-C3G mixed with different concentrations of Zn^{2+}-Cd^{2+}.

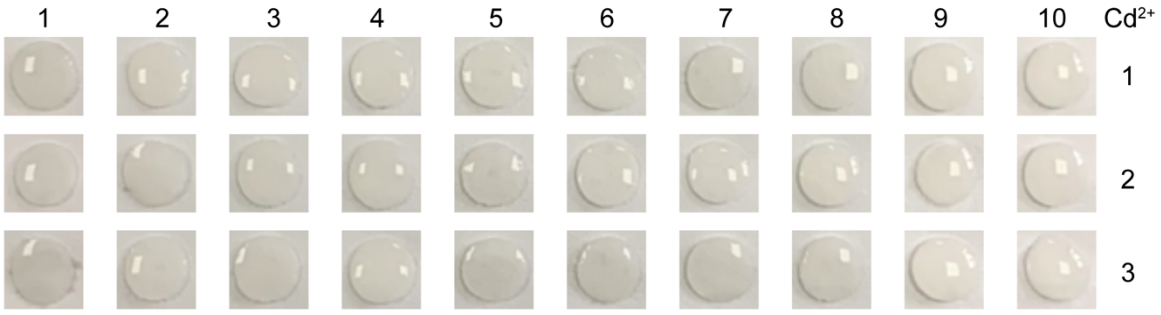

Fig. S42 Images of filter paper after mixing with different concentrations of Cd^{2+}.

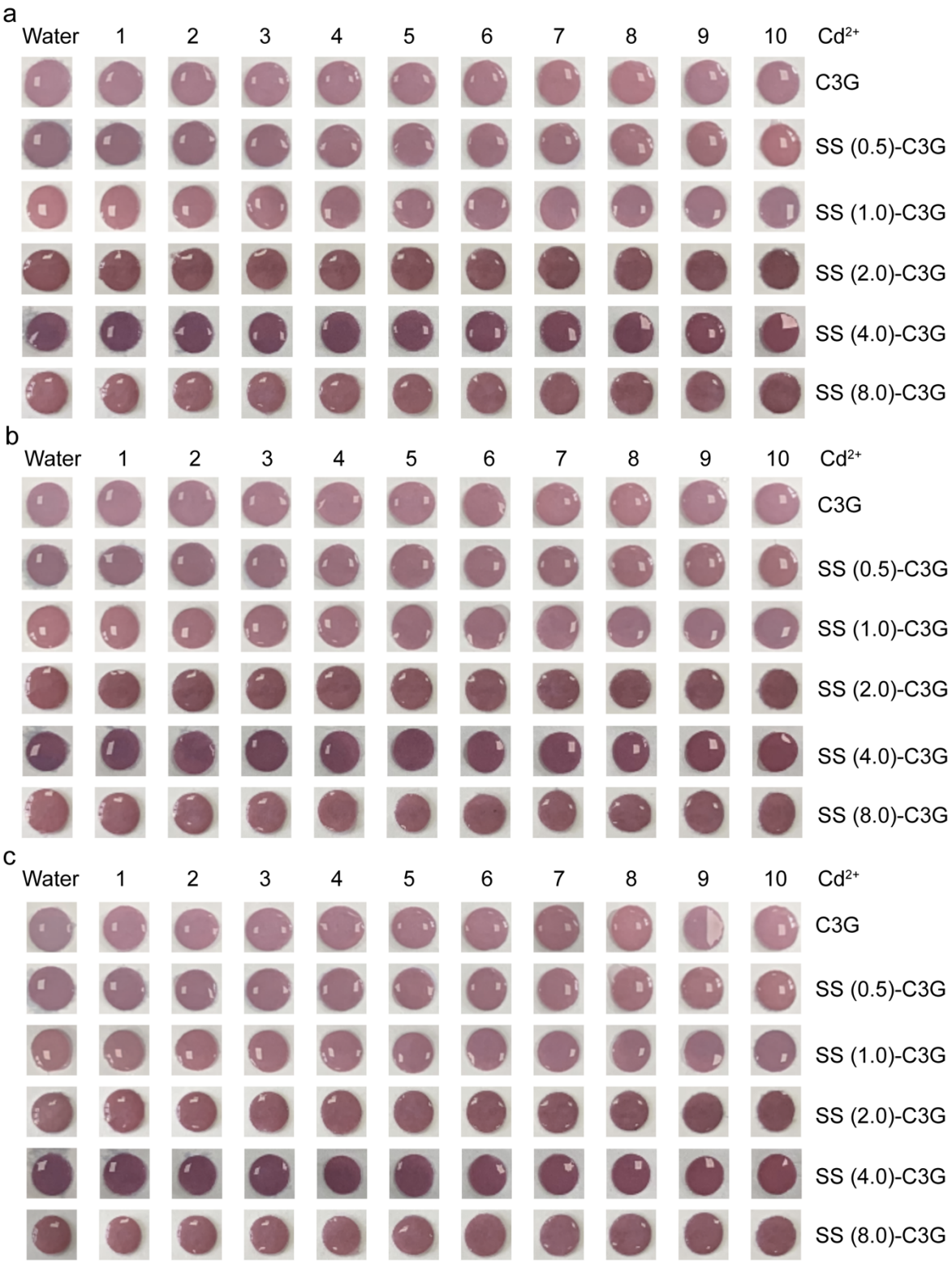

Fig. S43 Images of C3G and SS-C3G nanocomplex films (filter paper) after mixing with different concentrations of Cd^{2+}.

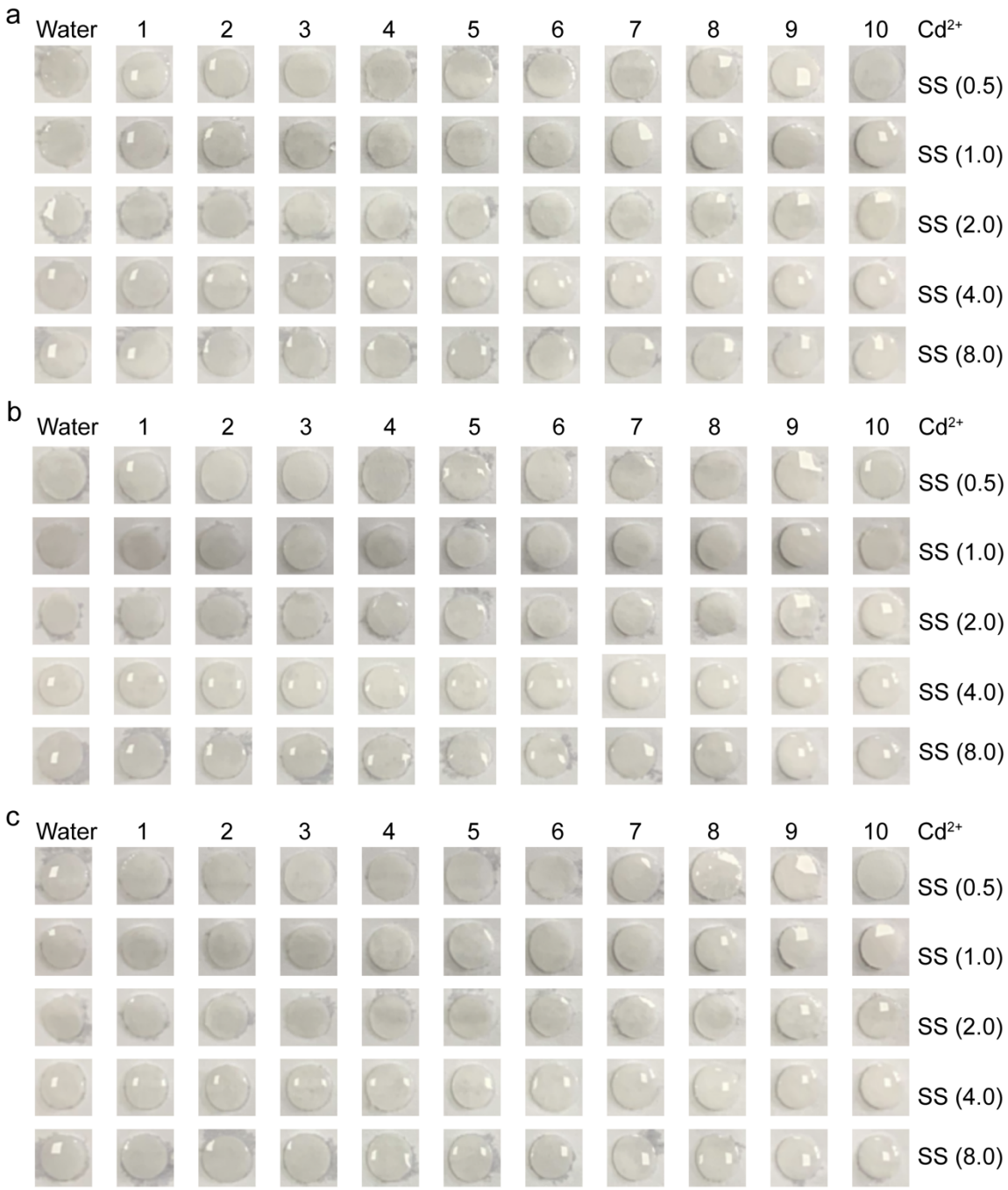

Fig. S44 Images of SS films (filter paper) after mixing with different concentrations of Cd^{2+}.

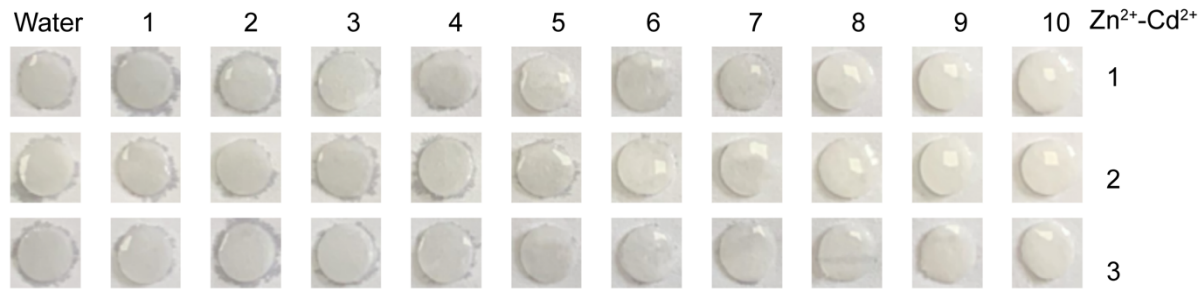

Fig. S45 Images of filter paper after mixing with different concentrations of Zn^{2+}-Cd^{2+}.

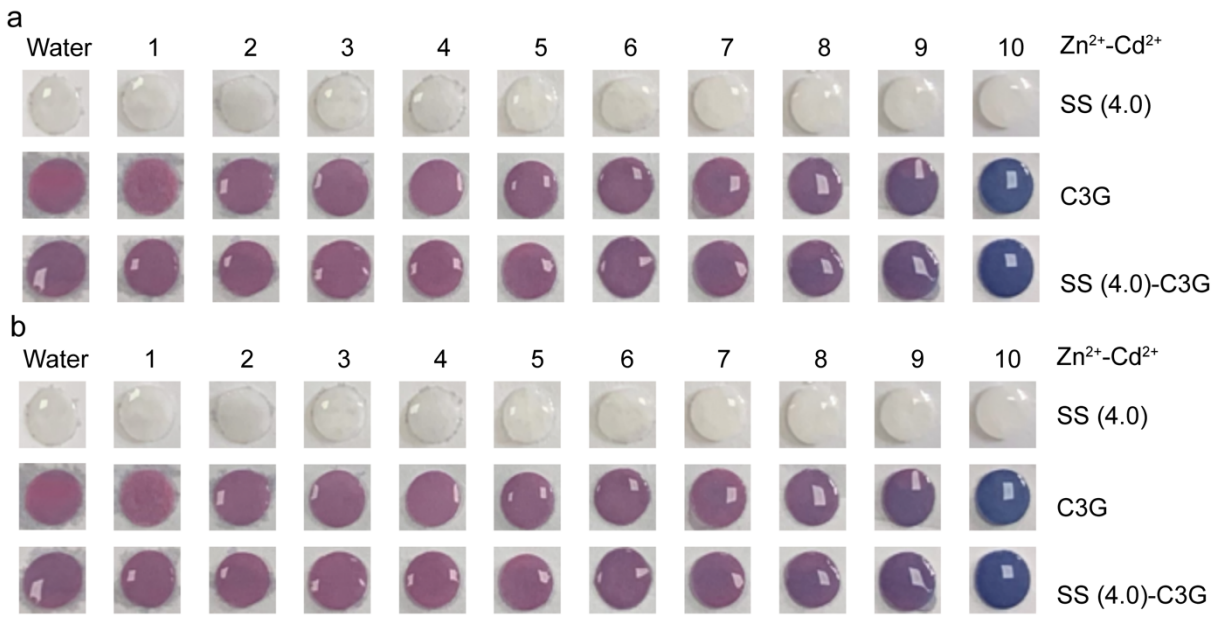

Fig. S46 Images of SS, C3G, and SS-C3G nanocomplex (filter paper) after mixing with different concentrations of Zn^{2+}-Cd^{2+}.